Firmato digitalmente da GIUNTINI GAIA C=IT

UNIVERSITÀ DI SIENA 1240

DIPARTIMENTO DI MEDICINA MOLECOLARE E DELLO SVILUPPO

DOTTORATO DI RICERCA IN

MEDICINA MOLECOLARE

CICLO XXXIV

COORDINATORE

Prof. Vincenzo Sorrentino

TITOLO DELLA TESI:

Investigating the Hedgehog pathway and Carbonic Anhydrase XII as prognostic and therapeutic targets of melanoma dissemination.

SETTORE SCIENTIFICO-DISCIPLINARE: BIO/09

DOTTORANDA:

Dott.ssa Gaia Giuntini

TUTOR:

Prof. Fabio Carraro

ANNO ACCADEMICO: 2021/2022

“Your courage is stronger than your fear”.

To you, mum.

Abstract

Malignant melanoma is the deadliest form of skin cancer and its tendency to easy migrate and give metastasis makes much more difficult its management. Several therapeutic strategies have been developed but long patient survival benefits reported widely range of chemoresistance. In this scenario, the Hedgehog (Hh) pathway, an essential pathway involved in embryonic development and aberrant re-activated in melanoma, may represent a promising therapeutic target. In primary melanoma Hh has been already investigated, but the mechanism by which the primary tumor disseminates and gives metastases has not been elucidated yet.

Tumor microenvironment (TME) is characterized by low O_2 levels (defined as intratumoral hypoxia), which contributes to cancer progression and poor prognosis. Within the TME, Carbonic Anhydrase XII (CAXII) plays pivotal roles in making the environment more acidic, allowing tumor cell adaptation and survival. Indeed, it represents a poor prognostic target for many tumors.

Recent studies correlated the Hh pathway and CAXII in breast cancer, but no evidence regards melanoma. For this reason, this thesis aimed to investigate whether a correlation between the Hh pathway and CAXII exists also in melanoma and if it may be responsible for melanoma motility. At this purpose, firstly transient silencing of Smoothened (SMO), glioma-associated oncogene protein 1 (GLI1) and CAXII were achieved, to study their role in migration and invasion in two malignant melanoma cell lines (SK-MEL-28 and A375) with different invasiveness capabilities; then two new designed SMO and GLI1 inhibitors were used, to deep understand the role of the two major factors of the Hh cascade in controlling melanoma migration via CAXII inhibition. Lastly, we also tested newly designed chemical compounds targeting Carbonic anhydrase IX (CAIX) and CAXII to evaluate them as possible new therapeutic agents for malignant melanoma. From this manuscript emerged that both SMO and GLI1 inhibition reduced melanoma cell migration, invasion and CAXII expression, under both normoxic and hypoxic conditions. Suppression of CAXII also resulted in decreased migration and invasiveness ability. Same results were confirmed by means of chemical compounds targeting the Hh cascade. Finally, I observed a more crucial role of CAXII rather than CAIX in controlling melanoma motility, as even a direct CAXII blockade resulted in impaired both cell migration and invasion under hypoxia. To conclude, this thesis brought out that CAXII plays crucial role in melanoma migration and invasion and its inhibition may be achieved with a direct or indirect, via Hh pathway, therapeutic approach.

Index

1. INTRODUCTION 7
1.1 MELANOMA 7
1.1.1 Epidemiology 7
1.1.2 Risk Factors 7
1.1.3 Molecular pathways on melanoma development 9
1.1.4 Molecular diagnosis of melanoma 9
1.1.5 Melanoma therapeutic strategies 10
1.2 THE HEDGEHOG PATHWAY 12
1.2.1 The canonical Hedgehog signal transduction 13
1.2.2 Non canonical Hedgehog signal transduction 15
1.2.3 Hedgehog and cell migration 16
1.2.4 Hedgehog in cancer 16
1.2.5 Hedgehog and melanoma 18
1.3 HYPOXIA AND HYPOXIA-INDUCIBLE FACTORS 19
1.3.1 Physiological feature of hypoxia 21
1.3.2 Pathological aspects of hypoxia 22
1.3.3 Role of hypoxia in melanoma 23
1.4 CARBONIC ANHYDRASES 25
1.4.1 Carbonic Anhydrases in cancer 26
1.4.2 CAIX 27
1.4.3 CAXII 27
2. AIM OF WORK 28
3. MATERIAL AND METHODS 29
3.1 Cell cultures 29
3.2 Hypoxic treatment 29
3.3 Transient transfection 30
3.4 Chemical compounds 30
3.4.1 Glabrescione B 30
3.4.2 Compound 22 30

3.4.3 GV2-20 31
3.4.4 Compound 7-10 31
3.4.5 Acetazolamide 32
3.4.6 Ara-C 32
3.5 Cell viability 32
3.6 Western blot 32
3.7 RNA extraction and RT-qPCR 33
3.8 Scratch assay 34
3.9 Modified Boyden chamber 35
3.10 Zymography 35
3.11 Spheroids 36
3.12 Statistical analyses 36
4. RESULTS 37
4.1 SMO and GLI1 transient silencing affected CAXII protein expression 37
4.2 SMO and GLI1 knock down impaired melanoma migration and invasion 41
4.3 CAXII silencing also impaired melanoma migration and invasion 43
4.4 Glabrescione B and Compound 22 as newly compound targeting the Hh pathway 46
4.5 GlaB and C22 impaired melanoma cell migration and invasion 48
4.6 SMO and GLI1 inhibition affected melanoma cell interaction 52
4.7 CAXII chemical inhibition impaired melanoma migration 53
4.8 CAXII chemical inhibition also reduced melanoma invasion under hypoxia 54
5. DISCUSSION AND CONCLUSION 57
6. ABBREVIATIONS 60
7. REFERENCES 62

1. INTRODUCTION

1.1 MELANOMA

1.1.1 Epidemiology

Skin cancers are the most common form of tumors affecting more than 40% of cases worldwide [1]. The three most common type of skin malignancy can be divided in two categories: non-melanoma skin cancer, represented by basal cell carcinoma (BCC) and squamous cell carcinoma (SCC), and malignant melanoma [1]. In this dissertation, I focused the attention on malignant melanoma.

The first description of melanoma was in the 5th century by Hippocrates of Cos [2] and since then many studies and discoveries have been emerged about this kind of malignance. Today, malignant melanoma is the less common among skin cancer, indeed it accounts only for 1% but represents the deadliest form, 80% of skin tumor deaths (https://seer.cancer.gov). Its incidence is increasing every year, predominantly in fair-skinned countries [3], and 99,780 new cases will be diagnosed in the United States in 2022 according to American Cancer Society's estimate.

1.1.2 Risk Factors

Melanoma takes its name and origin from melanocytes. Physiologically, melanocytes take place at the basal level of the epidermis and produce the melanin pigment. After exposure to ultraviolet radiation (UVR), keratinocytes produce α-melanocyte stimulating hormone (α-MSH), which binds the melanocortin 1 receptor (MC1R) on melanocytes, thus stimulating melanin synthesis. Then, the melanin is transported into surrounding keratinocytes through finger-like projections. When exposed to sun light, keratinocytes accumulate melanin, which protects their nuclei from UVR mutagenic effects. When keratinocytes mature and die, the outer layer of the skin is stained and protected by both melanin pigment accumulated in keratinocytes and a layer of dead keratinocytes (**figure 1**) [4, 5].

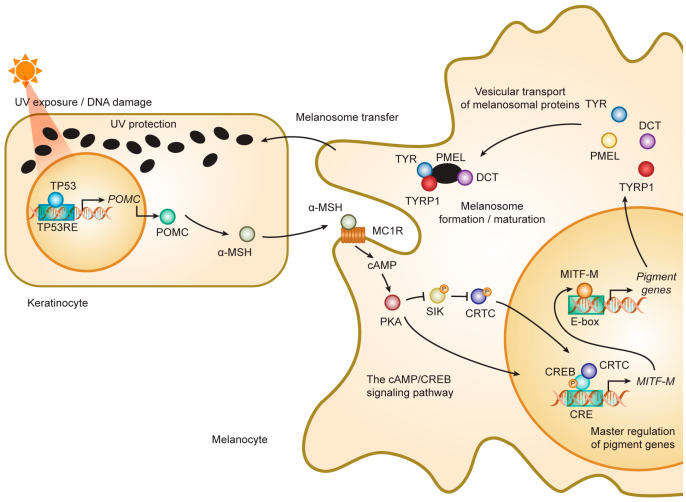

Figure 1: melanogenesis cascade in human skin [6].

Malignant transformation of melanocytes leads to melanoma development. UVR exposure represents the most critical environmental risk factor [7]. Thus, UVR generate mutations on DNA, especially on cytosine, which is more susceptible to UV-A rays, inducing the C>T transition that represents the typical UVR-induced mutational signature [8].

Moreover, number of nevi, genetic susceptibility, and family history present also relevant risk factors for the melanoma genesis. Thus, 25% of cutaneous melanoma develops from nevi [9], whereas polymorphisms of MC1R gene represent the most frequent cases for melanoma susceptibility [10]. 5-15% of cases accounts in family history and hereditary melanomas are less common, but germline mutations in cyclin-dependent kinase inhibitor 2A (CDKN2A) or in cyclin-dependent kinase 4 (CDK4) are the most frequent [11]. Eventually, other inherited conditions, as familial retinoblastoma, xeroderma pigmentosum and Li–Fraumeni cancer syndrome, seem to be also related to an increased risk of melanogenesis [12].

1.1.3 Molecular pathways on melanoma development

However, UVR are not only responsible for DNA mutations, but they have also tumorigenic effects, modulating signaling pathways involved in the onset, proliferation, survival, progression, and invasion; thus, for example, UVR are responsible for increasing the secretion of gamma interferon (IFN-γ) [13] or for the activation of C-Jun N-terminal kinase (JNK) signaling [14]. Nevertheless, somatic mutations are often responsible for melanoma genesis, progression and also response to therapy [8]. Numerous oncogenic mutations in melanoma occur within known signaling pathways. The most common of these is BRAF-V600E, which occurs in approximately 60% of melanomas [15]; also activating KIT aberrations are frequent, along with in/activation of NRAS, KRAS,MEK, CDNK2A deletions, PTEN disruptions and PI3K/AKT activations [15, 16] (**figure 2**).

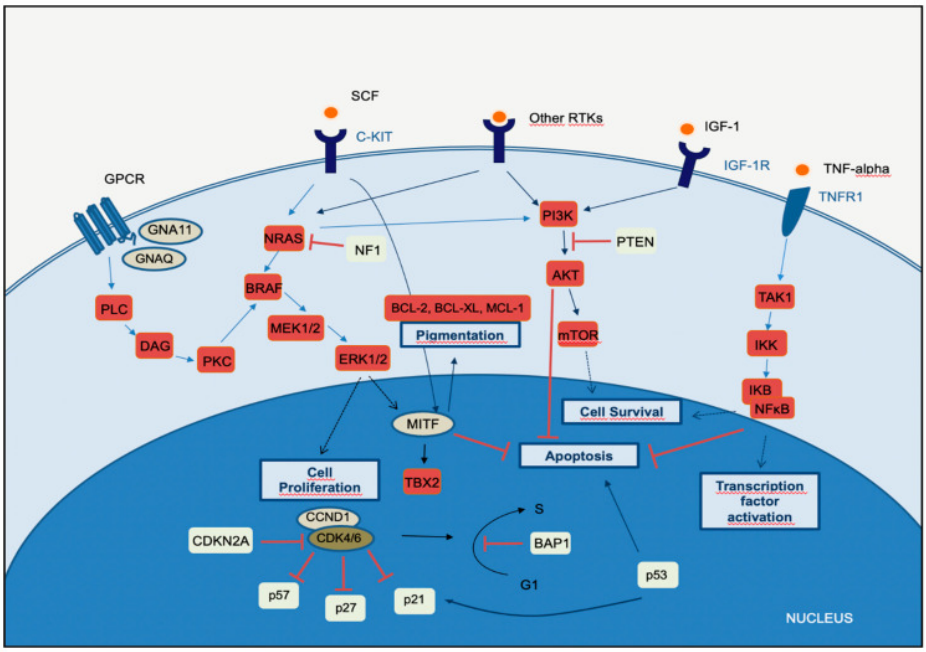

Figure 2: melanoma key signaling pathways [17].

1.1.4 Molecular diagnosis of melanoma

Crucial aspect for the diagnosis of a melanocytic skin lesion is the integration of several histopathological criteria with the clinical features. However, in many cases general morphological criteria are difficult to apply, especially in non-highly recurrence lesions, and so, the classical classification of melanocytic tumors might no longer be the proper approach. Thus, The World Health Organization (WHO) in 2018 indicated nine pathways associated with melanoma, each with specific genetic drivers (**table 1**) [18].

Relationship with sun exposure/damage	*Subtype*	*Genetic hallmarks*
Melanoma arising in sun-exposed skin.	*Low-CSD melanoma/superficial spreading melanoma.*	High frequency of BRAF p. V600 mutations.
	High-CSD melanoma (including lentigo maligna melanoma and high-CSD nodular melanoma).	Predominating mutually exclusive NF1, NRAS, other BRAF (non-p. V600E), and perhaps KIT mutations.
	Desmoplastic melanoma.	Recurrent inactivating NF1 mutations, NFKBIE promoter mutations, and several different activating mutations in the MAPK pathway (e.g. MAP2K1)
Melanoma arising at sun-shielded sites or without known etiological associations with UV radiation exposure.	*Malignant Spitz tumor (Spitz melanoma).*	Mutations in HRAS and kinase fusions in ROS1, NTRK3, ALK, BRAF, MET, and RET; CDKN2A homozygous deletion, TERT promoter mutations and MAP3K8 fusions/truncating mutations only in aggressive or lethal variants.
	Acral melanoma (including nodular melanoma in acral skin).	Multiple amplifications of CCND1, KIT, and TERT; mutations of BRAF, NRAS, and KIT; kinase fusions of ALK or RET in a few cases.
	Mucosal melanoma.	Numerous copy number and structural variations; uncommonly, KIT and NRAS mutations.
	Melanoma arising in congenital nevus.	In large to giant congenital nevi: NRAS mutations; in small to medium-size congenital nevi, BRAF mutations.
	Melanoma arising in the blue nevus.	Initiating mutations in the Gaq signalling pathway (GNAQ, GNA11, CYSLTR2, PLCB4); monosomy 3 (associated with loss of BAPI) and chromosome 8q gains in aggressive cases; additional secondary copy number aberrations in SF3B1 and EIFIAX.
	Uveal melanoma.	Mutually exclusive mutations in the Gaq pathway (GNAQ, GNA11, CYSLTR2, PLCB4); BAP1, SF3B1, and EIFIAX mutations during progression.

Table 1: schematic World Health Organization (WHO) 2018 melanoma classification, according to the involved pathways.

Of course, to minimize diagnostics ambiguities and follow WHO 2018 indications, histological evaluation should be accompanied by basic immunohistochemistry (IHC) and molecular tests. Recent recommendations of the European Organization for Research and Treatment of Cancer, the European Society of Pathology, and the EURACAN for the diagnosis of intermediate melanocytic proliferations and melanoma variants indicate that laboratories should perform basic IHC tests, such as: HMB-45; SOX10; MITF, tyrosinase, MART-1; P16; Ki-67/MIB1; BAP1 (BRCA1-associated protein 1); β-catenin; PRAME; and at least one molecular method to detect BRAF codon 600 and NRAS mutations [18].

1.1.5 Melanoma therapeutic strategies

As mentioned above, the most important therapeutic target is BRAF and the most frequent genetic alteration is BRAFV600 (with many difference variances as BRAFV600D/E/G/K/M) [19].

This is the reason why MAPK signaling pathway has become the most investigated for target therapy in melanoma patients. The Food and Drug administration (FDA) approved BRAFV600E/K inhibitors (BRAFi; vemurafenib and debrafenib as first-line treatment), MEK1/2 inhibitors (MEKi), and dual-MAPK pathway inhibition with BRAFi and MEKi combination for patients with BRAFV600E/K mutation, both in unresectable or metastatic melanoma (**figure 3**) [17]. In addition, larotrectinib and entrectinib are approved for patients with solid tumors which present NTRK gene fusions [17]. Importantly, BRAFi lead to characteristic side effects, which limit treatment and favor the development of chemoresistance through the upregulation of RTKs or NRAS [20]. However, preclinical data reported that BRAFi-resistant patients were sensitive to MEKi; thus the combination of BRAi plus MEKi seem to be promising, as it decreased the side effect and increased free survival rate and overall survival. Therefore, this dual chemotherapy was evaluated in clinical studies, but to date no adequate direct comparison has been performed in randomized trials [17].

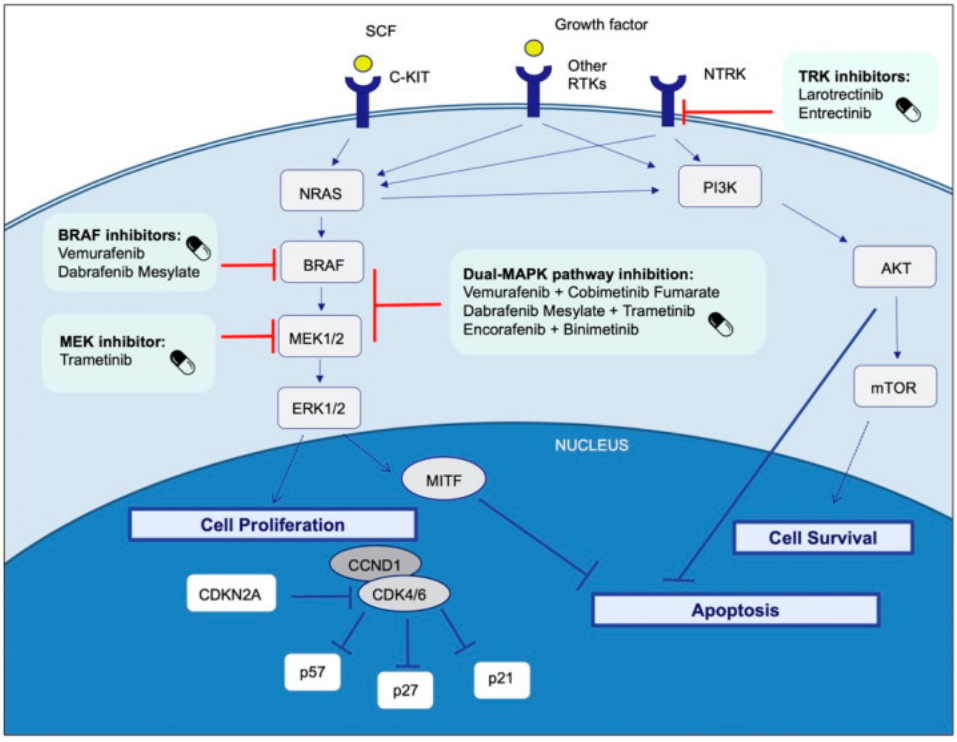

Figure 3: Melanoma Food and Drug Administration (FDA)-approved target therapies [17].

In the context of other gene alterations, monoclonal antibodies against the protein 4 associated with cytotoxic T lymphocytes (CTLA-4) and programmed cell death-1 (PD1) were evaluated in clinical trials. However, free survival rate for patients treated with these immune checkpoint

inhibitors (ICIs) was poor and tumors progressed [17]. Recently, in the field of personalized immunotherapy, adoptive cell therapy (ACT) has been identified as a method to provide a long-lasting and effective response in melanoma [21]. Thus, ACT is designed to redirect host lymphocyte cells against tumor cells, using different strategies: tumor-infiltrating lymphocytes (TILs), T cell receptor-engineered T cells (TCR-T), and chimeric antigen receptor T cells (CAR-T) [17]. Finally, analysis of CRISPR-CAS9 screens has identified genes that have not been associated with melanoma, which can be targeted using available inhibitors, thus opening new treatment strategies that may be explored as potential therapeutic targets [22].

1.2 THE HEDGEHOG PATHWAY

Hedgehog (Hh) is an evolutionary conserved signaling pathway discovered in the fruit fly *Drosophila Melanogaster* by Nüsslein-Volhard and Wieschaus in 1980 [23]. It plays a pivotal role in embryonic development, regulating cell growth, cell cycle, cell lineage and differentiation, tissue patterning and organogenesis. Particularly, in human it plays crucial role in the development of brain and spinal cord, where in the last case, it is responsible for determining the dorso-ventral position of the neural tube [24, 25]. Later in life, the Hh pathway remains dormant, except in case of homeostasis regulation and stem cells maintenance in some tissues [26], as brain [27], skin [28], prostate [29] and bladder [30].

In humans, the Hh signaling is activated by three different Hh ligands, termed Sonic Hedgehog (SHH), Indian Hedgehog (IHH) and Desert Hedgehog (DHH). SHH and IHH have important functions in several tissues, especially SHH in nervous system cell type specification and limbs patterning and IHH in bone and cartilage development. DHH is restricted to the gonad formation [31-33]. Nevertheless, SHH is the best studied along ligands for his major involvement in development and cancer.

Hh ligands are synthetized in the endoplasmic reticulum (ER) as 45-kDa inactive precursor proteins, which undergo catalytic cleavage at the C-terminal (HH-C), with its consequent degradation by proteasome (**figure 4**). The N-terminal unit (HH-N) of 20 kDa undergoes a covalent attach of a cholesterol to the HH-C and a palmitoylation of the last cysteine at the HH-N [34, 35]. The lipid modification seems to play an important role in the integration of Hh ligands into the cell membrane by limiting their spread throughout the tissue [36]. Hh ligand releasing may occur in many different types: 1) it can be facilitated by the synergic action of the 12-pass transmembrane

Dispatched (DISP) and the secreted glycoprotein Scube2 as soluble monomers; 2) they can form soluble multimers; 3) they can associate with apolipoproteins; or 4) they can be released on the surface of exosomes [37].

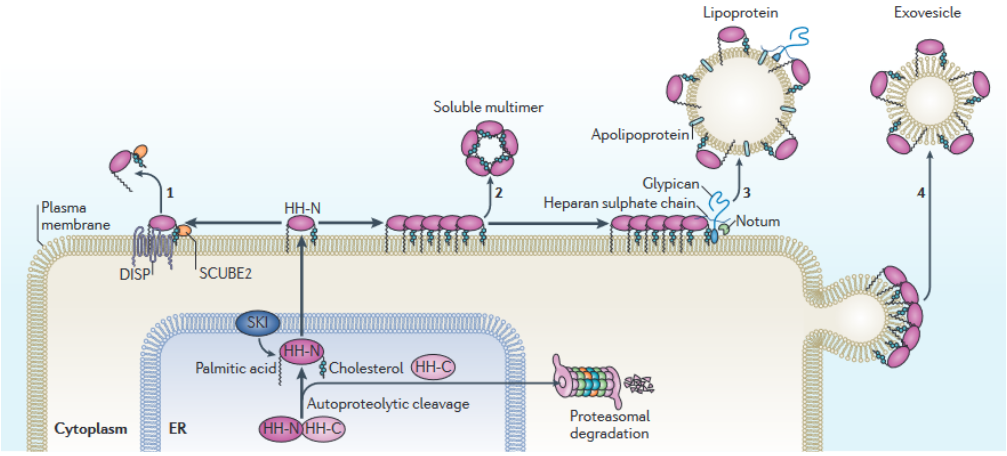

Figure 4: Hedgehog protein biogenesis and release [37].

1.2.1 The canonical Hedgehog signal transduction

The Hh signaling is propagated by the 12-pass transmembrane Patched (PTCH1 and PATCH2), and the 7-pass G-protein coupled receptor (GPCR)-like Smoothened (SMO) [38]. In the absence of Hh ligand (**figure 5**), PTCH1, which is located at the base of the primary cilium (PI), a hair-shaped microtubule-based organelle, catalytically represses SMO, which is internalized within intracellular vesicles, preventing its localization to the membrane. In this phase, glioma-associated oncogene protein 1 (GLI1) is not expressed, since it acts just in the activator form, whereas GLI2-3 are complexed with Suppressor of Fu (SuFu) and the Kinesin family member 7 (KIF7) shuttles the SuFu-GLI2-3 complex to the ciliary tip by the intraflagellar transport system (IFT). Therefore, kinase A (PKA), casein kinase 1α (CK1) and glycogen synthase kinase 3β (GSK3β) phosphorylates the full length GLI2-3, promoting their proteolytic cleavage and consequent removal of their “activator” domain, generating GLI2R and GLI3R, that act as repressor of the nuclear transcription of Hh target genes [37-39].

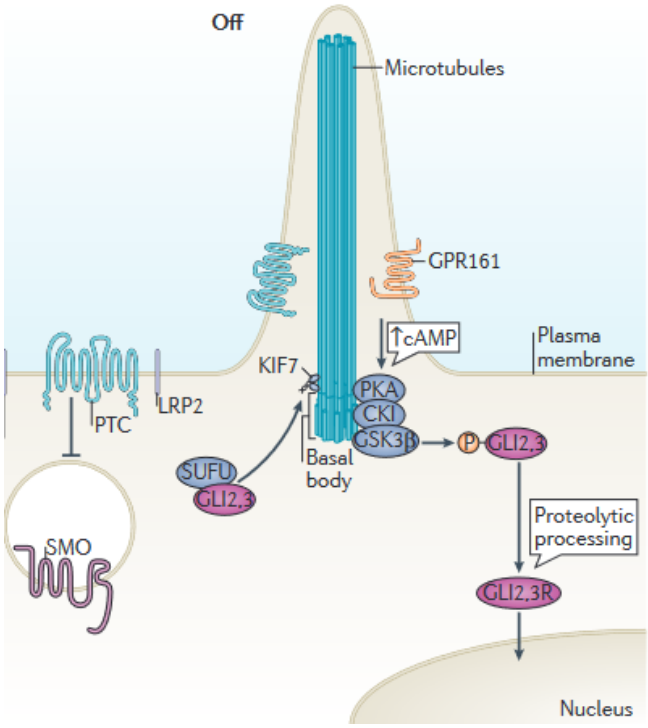

Figure 5: Hh signaling in absence of Hh ligand (modified from Brisco et al., [37]).

On the contrary, when the Hh ligand binds to PTCH (**figure 6**), the complex Hh-PTCH is internalized and undergoes proteasomal degradation. In this way, SMO can be phosphorylated by GPRK2 and CKI, which block its internalization, as well as stabilize its active conformation to promote its translocation to the PI. Within the PI, SMO antagonized with SuFu activity, thereby promoting GLI2-3 dissociation from SuFu-GLI2-3 complex and facilitating the releasing of GLI activator (GLIA) [40, 41]. Consequently, GLIA translocates into the nucleus to trigger the transcription of HH target genes, which are involved in processes such as proliferation (D-type Cyclin1/2, CCDN1/D2), cell cycle (MYC), apoptosis (Bcl-2) and epithelial-to-mesenchymal transition (FOXC2, SNAI1, TWIST2), as well as regulating the Hh signaling *GLI1* and *PTCH1* genes [37, 39, 42].

The activated Hh pathway generates a feedback loop, which modulates the response of the receiving cell. Thus, the activation or inactivation of the Hh pathway is due to a balance between GLIA and GLIR [36].

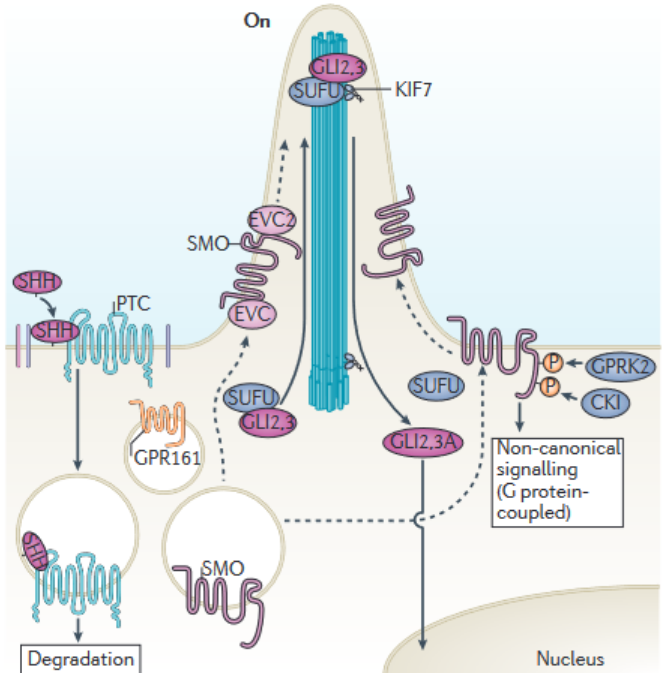

Figure 6: Hh signaling in presence of Hh ligand (modified from Briscoe et al., [37]).

1.2.2 Non canonical Hedgehog signal transduction

While the canonical signaling transduces via Hh/PTCH/SMO/GLI route, a plethora of different pathways have been documented to be activated independently from GLI1-induced transcriptional changes and research community recognizes these activations as “non-canonical Hh signaling” [37, 43]. More specifically, non-canonical Hh signaling currently refers to Hh co-receptor which initiate the signal cascade bypassing GLI1 activity (**figure 7**) [44].

Thus, non canonical Hh signaling pathway can be classified into three groups: *Type I* signals, that trigger exclusively from PTCH activation by the ligand and are involved in proliferation and apoptosis; *Type II* signals (also termed SMO-dependent, GLI-independent), that stem from SMO activation and are involved in metabolism, cytoskeleton rearrange e migration; lastly, *Type III* signals are represented by SMO-independent-GLI dependent signalings [44, 45]. However, despite the classification of the different natures of the non canonical cascade, still many points of these mechanisms need to be defined [45].

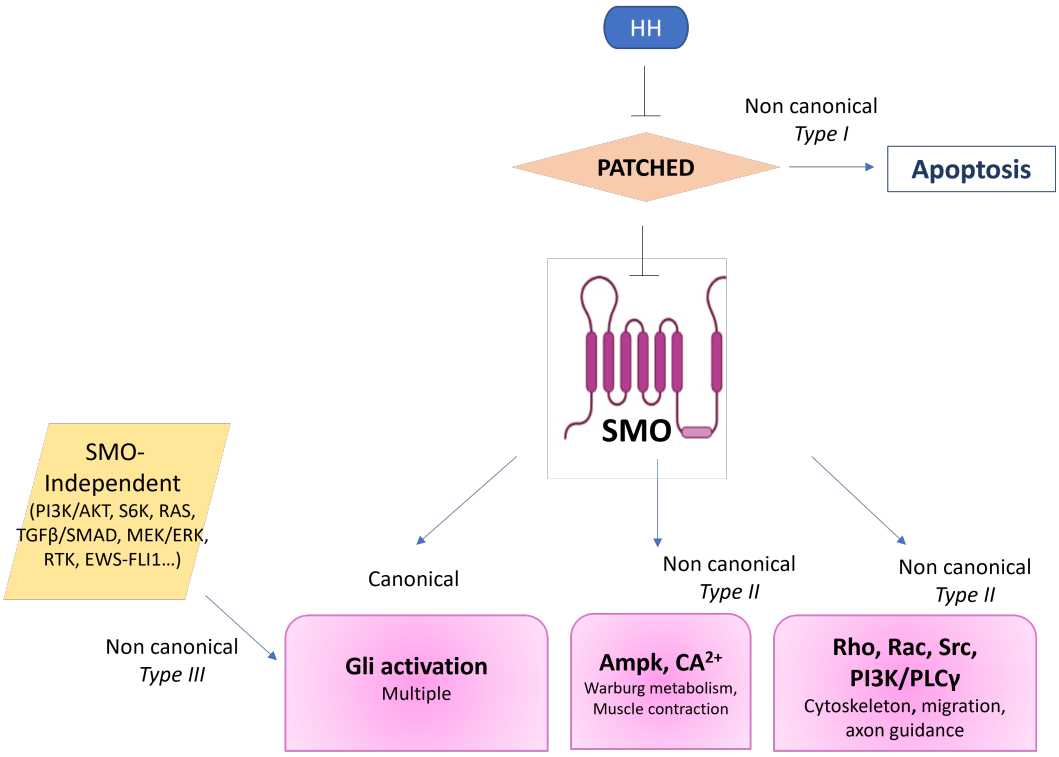

Figure 7: Schematic illustration of non canonical Hh signalings.

1.2.3 Hedgehog and cell migration

Cell migration is a widespread and complex cellular activity fundamental in several biological processes, as embryonic development and tumor infiltration and dissemination. As individual or groups, cells migrate toward their target sites by the guidance of specific molecules, which act mainly regulating cytoskeletal arranges and membrane dynamics [46]. Conversely, as a morphogen, Hh controls cell migration by inducing transcriptional changes in its target genes, that are involved in the acquisition of mesenchymal feature (defined as “epithelial-to-mesenchymal (EMT) transition) and migration. Therefore, Hh signals induce EMT via SNAI1, SNAI2, ZEB1, ZEB2, TWIST 2 and FOXC2 regulation [47]. In addition, it is documented that Hh enhances migration and metastases, promoting cell adhesion via focal adhesion kinase (FAK) regulation [48]. Lastly, it is known that SHH induces the formation of lamellopodia in fibroblasts, promoting cell migration through G-protein-dependent activation of RhoA and Rac1 [49].

1.2.4 Hedgehog in cancer

Not surprisingly, due to Hh involvement in several functions, defects on its signaling are correlated to numerous human disorders, such as birth defects and cancer [24].

The first indication of Hh pathway in cancer was in 1987 when Kinzler et al., discovered a gene amplified more than 50-fold in malignant gliomas; that gene was therefore termed GLI1 [50]. Since that discovery, many Hh elements have been identified and now it is known that deregulation of any component of the Hh cascade leads to its aberrant activation, resulting in malignant transformation. Indeed, according to the latest estimates, Hh pathway aberrations occur in 25% of all human cancer and its anomalous activation can be both ligand-independent or -dependent [51]. Thus, three different mechanisms of aberrant Hh signaling activation have been identified in cancer (**figure 8**):

- Type I- ligand-independent: this type of Hh activation includes loss-of-function PTCH1 or SuFu mutations or SMO activating mutation, thereby it can no longer be inhibited by PTCH1. The final result is a constitutive activation of Hh cascade in the absence of the ligand. This kind of Hh aberrant activation is mostly observed in BCC, medulloblastoma and rabdomyosarcoma [42, 51].
- Type II- ligand-dependent autocrine/juxtacrine signaling: the tumor cell secretes the Hh ligand, which can be internalized in an autocrine manner or taken up into the nearby tumor cells (juxtacrine manner), thus activating the signal cascade promoting tumor cell survival and proliferation. This kind of mechanism was observed in tumors, as stomach, pancreatic, colorectal, ovarian and endometrial, breast, prostate, and melanomas [42, 52].
- Type IIIa - ligand-dependent paracrine signaling: tumor cells secrete the Hh ligand which stromal cells internalize. Then, the stimulated stromal cells respond secreting vascular endothelial growth factor (VEGF) and insulin-like growth factor (IGF), which stimulate and support survival and growth of tumor cells. This kind of mechanism resembles the physiological activation of the Hh pathway during the development of the embryo [53].
- Type IIIb - Ligand-dependent reverse paracrine signaling: stromal cells secrete the Hh ligand which is directly taken up by the tumor cells. Also in this case, the ligand supports tumor proliferation and growth. This mechanism was described in case of lymphomas and multiple myelomas [51, 53].

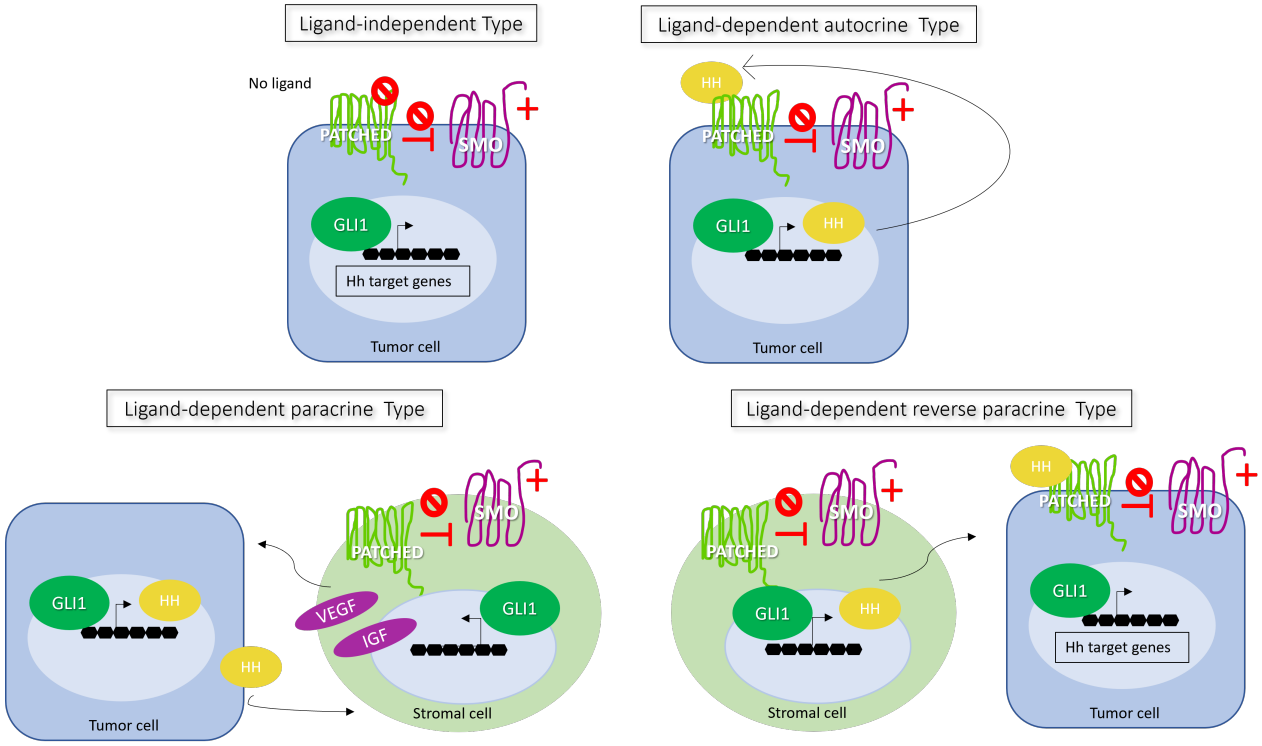

Figure 8: Schematic mechanisms of the activation of Hedgehog signaling in cancer.

1.2.5 Hedgehog and melanoma

While abnormalities of the Hh signaling are related to the onset and development of several tumors, the effects of this pathway in melanoma are still unclear. Some studies reported that downregulation of GLI1 results in inhibition of melanoma proliferation and increasing of cell apoptosis [54, 55]. Moreover, it is demonstrated that SMO/GLI1 downregulation are responsible for decreasing melanoma cell migration and mesenchymal transformation capabilities [55]. Furthermore, Chen et al., demonstrated that the activation of Hh/GLI1 enhances MYC-activated Cyr61 expression, boosting the metastasis formation [56]. Although mechanisms involving the Hh pathway in melanoma remain still unexplained, there is sufficient evidence to investigate it as a possible therapeutic target for melanoma management.

1.3 HYPOXIA AND HYPOXIA-INDUCIBLE FACTORS

Metazoan life is oxygen (O_2) dependent for carrying out essential metabolic processes, like respiration [57]. Indeed, thanks to the atmospheric O_2, which is absorbed by lung and exchanged in bloodstream with carbon dioxide (CO_2), oxidative phosphorylation (OXPHOS) process transforms the energy stored in carbon bonds of carbohydrates and fatty acids in high energy adenosine triphosphate (ATP), which is used as currency in several physicochemical reactions in living cells [58]. This metabolic activity occurs in mitochondria in presence of normal level of molecular O_2 and is responsible for 90% of its consumption [59]. Consequently, a drop of tissue O_2 levels arises and storage of non-mitochondrial O_2 is used to maximize ATP production and activate alternative pathways; nevertheless, when demand exceeds supply, a state of hypoxia is established [60]. During evolution, mammalian cells evolved an efficient molecular response system, which senses the O_2 variations and leads cells to adaptation. The master regulators of the adaptive O_2 variation are the hypoxia-inducible factors (HIFs). HIFs is a family of heterodimers consisting of an hypoxically inducible alpha subunit (HIF-α) and a constitutively expressed beta subunit (HIF-β) [59, 61]. The first HIF discovered was HIF-1 by Gregg L. Semenza during its studies regarding erythropoietin (EPO), which earned him the Nobel prize for Medicine in 2019. Starting from its discovery, HIF-1α became the most studied and well-characterized factor within the HIF family [62]. Now it is well known that HIF-1α (120 kDa) heterodimerizes with HIF-1β (91-94 kDa) to form HIF-1 complex, which binds target gene promoters to the 50-base pair Hypoxia Responsive Elements (HREs)-DNA motif, acting as their transcriptional factor [63]. Other two HIF-α isoforms exist in human, HIF-2α and HIF-3α but only HIF-1α is ubiquitously expressed in all human cells [64].

HIF-1α transcriptional activity is tightly regulated by oxygen availability (**figure 9**): indeed, under normoxia prolyl hydroxylases 1-3 (PHD1-3) and factor inhibiting HIF (FIH) hydroxylate α subunit of HIF-1, blocking its interaction with activators as CBP/p300; in the meanwhile, von Hippel-Lindau protein (pVHL) assemblies the complex VHL-Elongin B, Elongin C-CUL2-RBX1, which together with ubiquitin-conjugated E2, accomplishes HIF-1α ubiquitination and proteasomal degradation [65, 66]. Conversely, under hypoxic condition, pVHL, PHDs and FIH resulted to be inactivated by the low O_2 tension and HIF-1α can escape from proteasomal degradation, enters the nucleus, where interacts with HIF-1 β, and then the whole complex binds the HREs motif on the DNA of the target genes, consequently activating their transcription process [66].

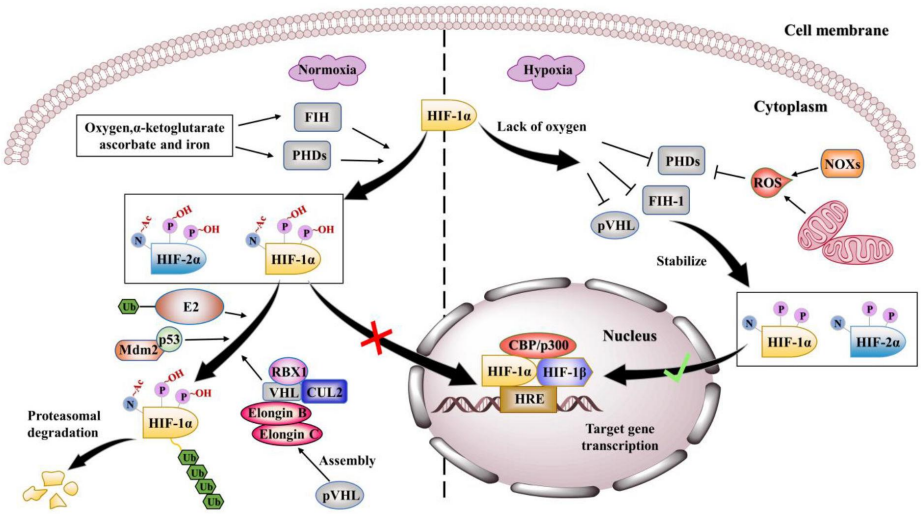

Figure 9: HIF-1α regulation according to O_2 availability [67].

To date, HIF-1 is responsible for the downstream of more than 100 targets, which resulted to be involved in several functions [66]. Within this context, it is well known that hypoxia enhances the expression of EPO, which increases the formation of red blood cells and, as a consequence, the delivery of O_2 to tissues [68]; therefore, HIF-1 activates the VEGF, which is the most potent endothelial-specific mitogen, to stimulate the proliferation of endothelial cells into hypoxic areas [69]. Moreover, HIF-1 also stimulates genes involved in maintaining vascular tone or governing matrix metabolism, as matrix metalloproteinases (MMPs) [70]. All detailed HIF-1 activated target genes are reported in **figure 10**.

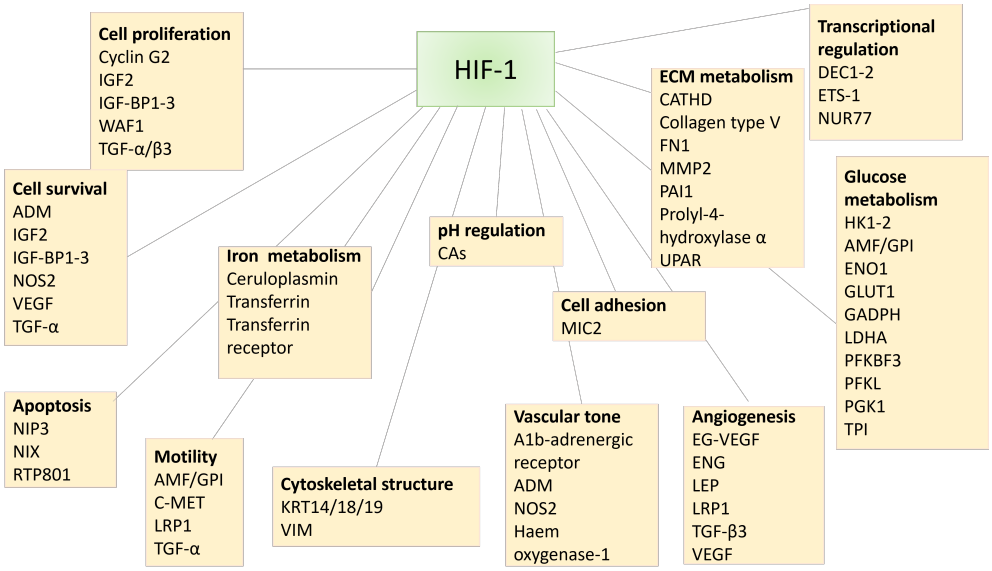

Figure 10: HIF-1 target genes.

1.3.1 Physiological feature of hypoxia

All human cells can sense O_2 changes and they can react to reduced availability within minutes (acute hypoxia), activating pre-existing proteins, or within hours (chronic hypoxia), through the regulation of gene transcription [71]. Besides, there are many causes that may compromise O_2 concentration and some of them occur even when lung is completely healthy; depending on the nature of the causes, we may classify 0_2 deprivation in physiological or pathological hypoxia. The most frequent case of physiological hypoxia is represented by high altitude: in this circumstance, the barometric pressure (which is 760 mmHg at sea level) decreases, even if the percentage of atmospheric O_2 remains constant, ~ 21 %, and consequently also the partial pressure of O_2 (pO_2) decreases (it is 159 mmHg at sea level and in the summit of Mount Everest it diminishes near 35 mmHg) [72, 73]. Not only that, but another example of physiological hypoxia is also represented by physical exercise; thus, with moderate physical activity, both O_2 consumption and CO_2 production increase, which in turn increase partial pressure of CO_2 (pCO_2); as a consequence, if the increased consumption of tissue O_2 isn't compensated by an enhanced perfusion, hypoxic state occurs and cardiac output and ventilation increase [74]. Moreover, there are some organs characterized by elevated O_2 consumption (and consequently live in an hypoxic state), due to their intense proliferation and consequent metabolic demand, as the spleen (where pO_2 corresponds to ~ 16 mmHg), thymus (pO_2 ~ 10 mmHg) [75], bone marrow (pO_2 ~ 0-30 mmHg) [76, 77] and lymph nodes (pO_2 ~ 16-40 mmHg) [78]. Lastly, hypoxia is fundamental in physiological processes (**figure 11**) such as the erythropoiesis, angiogenesis, the maintenance of immune cell homeostasis, the control of hematopoietic stem cell quiescence or self-renewal and the antibody production [79].

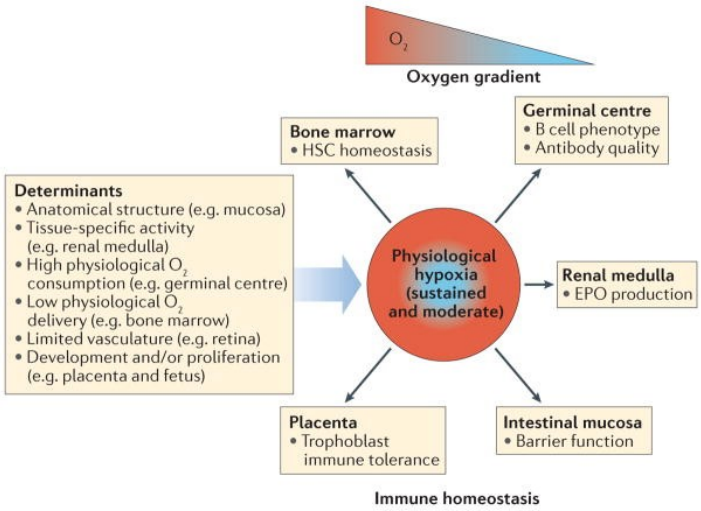

Figure 11: schematic representation of physiological hypoxia [79].

1.3.2 Pathological aspects of hypoxia

Pathological hypoxia occurs when a pathological process alters the normal diffusion or use of O_2. The most well studied pathological condition to be associated with hypoxia is cancer. Hypoxia can influence malignant cells by acting as a stress factor, inducing cell cycle arrest, apoptosis, necrosis or slowing proliferation; all these conditions may consequently favor tumor onset, progression and metastasis. Tumor mass contains typical hypoxic regions, due to the high rate of cell proliferation, together with structurally and functionally abnormal vascular architectures [80]. Thus, the vascular system built by the hypoxic tumor is messy, leaky, and inefficient in providing O_2 supply [81].

The relevance of hypoxia in neoplasms has been highlighted during the years thanks to studies showing that high HIFs levels are linked to a poor prognosis in cancer patients. Indeed, increased HIF-1α or HIF-2α levels in diagnostic tumor biopsies were associated with increased risk of mortality in cancers, as bladder, brain, breast, colon, cervix, endometrium, head/neck, lung, ovary, pancreas, prostate, rectum and stomach [66].

Another pathological condition characterized by hypoxia is ischemia. Ischemia occurs when O_2 and nutrient supply suddenly exceeds demand and it can be caused by arterial stenosis or acute blockage, rendering the tissue deprives of fundamental elements, such as O_2 and nutrients [58]. Of interest, ischemic tissue can produce chemotactic proteins that promote the migration of monocytes, which can contribute to angiogenesis through the production of pro-inflammatory cytokines with angiogenic properties [58]. Indeed, in tissue ischemia, two important conditions coexist: hypoxia and inflammation, that are considered fundamental stimuli for angiogenesis. This highly controlled process is associated with pathological conditions such as tumor growth, diabetic retinopathy, ischemic diseases and obesity [82, 83].

Moreover, hypoxia has found also in diseases where a lack of blood supply in tissue occurs, such as myocardial infarction, atherosclerosis, stroke, or preeclampsia, caused by placental hypoxia [84].

Eventually, chaotic and sever O_2 deprivation may be revealed in immunological niches, where it can be correlated to immune cell dysfunction. Indeed, it was already documented that high levels of immune activity runs parallel with tumor, inflammation, infectious and ischemic tissue. Indeed, chronic inflammation in immunological niches is often associated with inflammation-driven carcinogenesis [79].

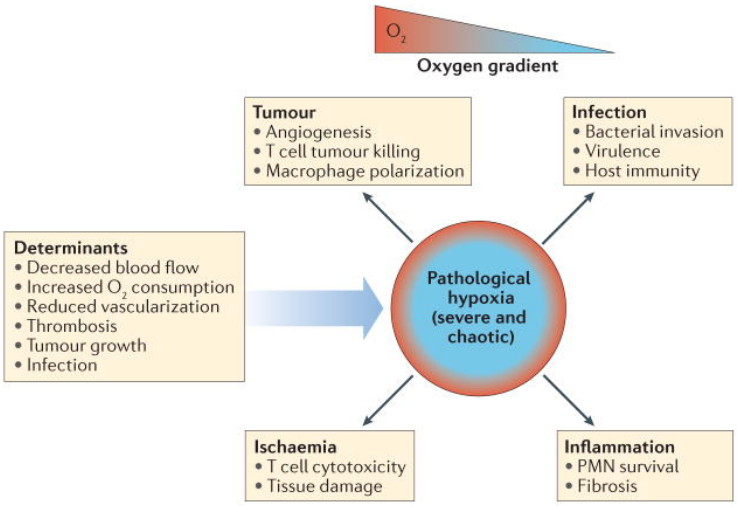

Figure 12: schematic representation of pathological hypoxia [79].

1.3.3 Role of hypoxia in melanoma

For skin tissue, the value of pO_2 varies from the well-oxygenated dermis to the modestly hypoxic epidermis, whereas portions of some sebaceous glands and hair follicles are moderately to severely hypoxic [85]. In melanoma, hypoxia represents a prevalent feature (**figure 13**). Thus, it is reported that upregulation of HIF-1α was detected both in primary and metastatic melanoma and its high expression is often associated with proliferative markers [86]; indeed, if the lack of O_2 often leads normal cells to apoptosis, hypoxia paradoxically frequently supports melanoma cell survival and it is associated with even more malignant phenotype (and poor prognosis for patients) [87]. For example, it is documented that a small non-coding microRNA, called miR-211, is able to sensitize melanoma cells to hypoxia-induced apoptosis; however, cancer cells lose its expression during melanoma development [88]. Furthermore, it is also shown that melanoma cells bearing BRAF V600E mutation exhibit downregulation of proapoptotic genes, as Bcl-2 associated agonist of cell death (BAD) and Bcl-2-like 1(BCL2L1) [89].

In general, hypoxia arises as a consequent of insufficient vascular architecture of intensively proliferating cancer cells. To avoid growth decreasing or even necrosis, tumor cells response to the hypoxic state inducing VEGFA and VEGFC expression, which trigger the formation of new vessels from preexisting ones. Elevated expression of VEGF and HIF-1α is frequently observed in melanoma [90], indicating that hypoxia in melanoma is also associated to enhanced angiogenesis [91]. However, melanoma cells are not the only source for proangiogenic factors in the tumor

microenvironment (TME), because tumor associated fibroblasts (also called CAFs) also secrete elevated level of VEGFA and Interleukin 6 (IL-6) when exposed to hypoxia [92].

Hypoxia has been repeatedly correlated with highly aggressive tumor behavior and aggressive cancers exhibit elevated plasticity, favoring their invasive ability. Thus, it is reported that hypoxic melanocytes harboring KIT mutation downregulate microphthalmia-associated transcription factor (MIFT), which is indicative of transcriptional reprogram aimed to induce a migratory phenotype [93]. Moreover, hypoxia is able to induce selection of cancer stem-like cells, which express self-renewable ability, enhanced invasiveness and elevated drug resistance. Li H., and colleagues reported that Nodal, one of the regulator of stemness, resulted upregulated under hypoxia and contributes to chemoresistance [94].

In addition, the loss of epithelial polarity and intracellular junction in favor of a mesenchymal phenotype (is that EMT phenomenon) influences melanoma cells to a high aggressive behavior. EMT process can be activated by Notch signaling or Snail1, which are promote by low O_2 state [95], along with other mesenchymal factors as N-cadherin, α-smooth muscle actin (α-SMA), SRY-box transcription factor 10 (SOX10) and simultaneous reduction of E-cadherin. [96].

Lastly, hypoxia also influences the interaction between melanoma cells and the extracellular matrix (ECM), which is essential for many processes, as adhesion, migration and invasion. Many reports describe that low O_2 levels increase the expression of cancer cell surface proteins, which act as receptors for soluble ligands or scaffold for the ECM molecules present in the TME [97-100].

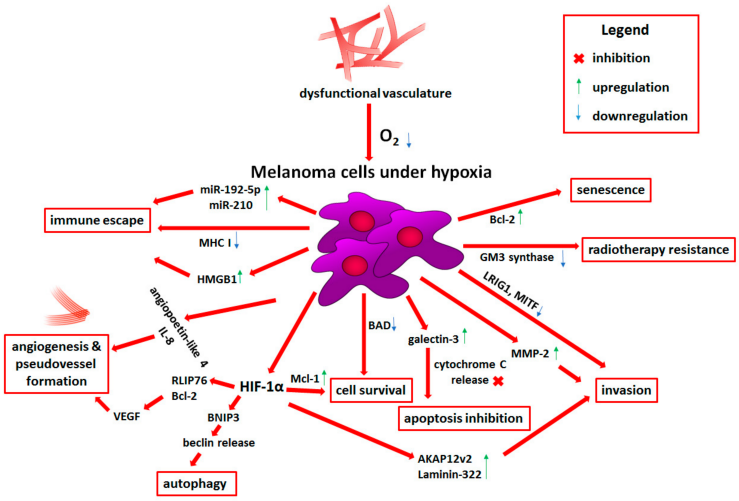

Figure 13: influence of hypoxia on melanoma [90].

1.4 CARBONIC ANHYDRASES

Firstly discovered in 1933, Carbonic Anhydrases (CAs) are a family of zinc-containing enzymes that catalyze the reversible hydration of carbon dioxide into bicarbonate and protons: $CO_2 + H_2O \leftrightarrow HCO_3^- + H^+$ [101]. They play crucial role in pH regulation; indeed, when intracellular CO_2, deriving as waste-product from cell metabolic activities, goes out the cell via aquaporin channels, it is converted into HCO_3^- by transmembrane CAs. Consequently, this reaction releases H^+ in the extracellular space that contribute to the acidification of pH. The generated HCO_3^- can be taken back into the cell by specific membrane transporters and it is now available for the hydration reaction by intracellular CAs (**figure 14**) [102]. Considering that CO_2 is the principal bioproduct of the oxidative process, with this mechanism CA activity is fundamental to maintain cell physiological processes, as respiration, electrolyte balance and biosynthetic reactions and bone remodeling. Furthermore, in the last years CAs have been extensively studied and many researchers demonstrated CAs involvement in tumorigenesis and cancer progression [101].

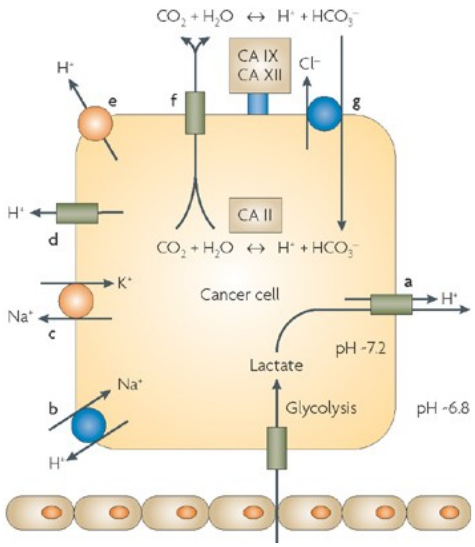

Figure 14: schematic representation of Carbonic Anhydrases (CAs) activity [102].

Six different CA families exist, which are organized in:

- αCA, expresses in vertebrates and algae;
- βCA, in plants and prokaryotes;
- γCA, in archaea;
- δCA and ζCA, express in marine diatoms;
- ηCA, in protozoa [103].

In human, 16 isoforms have been described [104] and, according to their subcellular localization, they can be divided in: cytosolic (CAI, CAII, CAIII, CAVII, CAVIII, CAX, CAXI, CAXIII), mitochondrial (CAVA, CAVB), secreted (CAVI) and membrane-associated (CAIV, CAIX, CAXII, CAXV, CAXIV) (**figure 15**) [103].

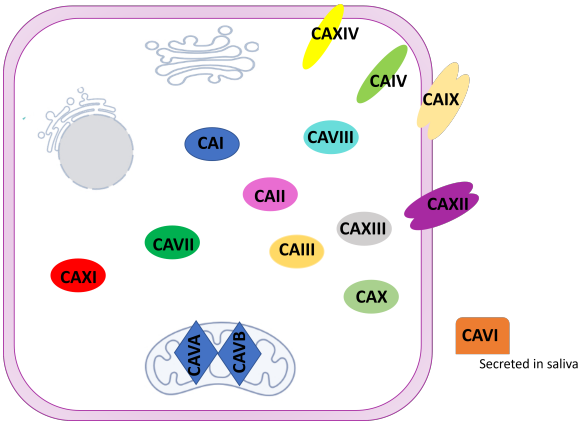

Figure 15: cellular localization of different CA isoforms.

1.4.1 Carbonic Anhydrases in cancer

Within the αCA family, CAIX and CAXII have gained a lot of interest in the scientific community for their involvement in cancer. Thus, these two enzymes result overexpressed in many cancer type and for this reason have been characterized as tumor markers in human cancer [105].

The expression of CAIX in normal tissues is restricted to the basolateral membrane of epithelial cells of the gastric, intestinal and gallbladder mucosa [106], whereas CAXII is much more widespread, but however its expression is higher in cancer than in normal tissues [107].

CAIX and CAXII distinctive feature is that their expression is triggered by hypoxia, thus they are known as hypoxia inducible genes [108]. Moreover, unlike CAIX, it is reported that the expression of CAXII is also strong correlated with estrogen receptor expression in breast cancers [109].

It was documented that they provide a conducive environment for tumor growth and spread, maintaining the extracellular acidic pH [108]. Not only that, but the acidification of the TME drives the metastatic phenotype of the tumor, with consequent cell migration, ECM degradation and invasion stimulation [110]. For this reason, CAIX and CAXII have become highly studied markers in tumors, both for prognostic and/or therapeutic value.

1.4.2 CAIX

This enzyme was discovered in human cervical carcinoma cells and originally named MN protein [111]. It is a homodimeric, transmembrane zinc metalloenzyme that dimerizes and undergoes post-transcriptional modifications [112]. The structure of CAIX can be distinguished in different domains: the extracellular portion, characterized by the single peptide (SP), proteoglycan (PG) and catalytic domains (CA). It seems that PG portion is responsible for cell adhesion, for maintenance of the catalytic activity and for the acidification of the TME [111].

There is a well-established role of CAIX in facilitating migration and invasion of cancer cells. Indeed, Radvak et al., reported that the suppression of CAIX gene in fibrosarcoma cells reduced the protein focal adhesions, resulting in a significant reduced spreading, migration and invasion [113]. Furthermore, CAIX is also an important component of invadopodia, F-actin-rich protrusions of the plasma membrane involved in ECM proteolysis and invasion [114]. Moreover, CAIX-embedded exosomes had shown to promote tube formation and migration of HUVEC cells *in vitro* [115]. Eventually, it is now established that overexpression of this protein is associated with poor prognosis for many tumors, as ovary [116], breast [117], bladder [118] and lung [119].

1.4.3 CAXII

Following initial CAXII discovery as tumor marker [120], its expression has been reported in different cancers [121], with higher expression in tumors than tissues [107].

CAXII expression in breast tumor is a good prognosis factor, as it is indicative of a lower grade disease, lower relapse rates and better overall survival [122]. Conversely, an alternative spliced variant of CAXII is expressed in brain tumors and associated with poorer prognosis [123].

In colorectal tumors, CAXII expression was found to increase with a high grade of dysplasia [124].

2. AIM OF WORK

Malignant melanoma is a fast-growing aggressive type of tumor and the deadliest form among skin cancers. After it metastasizes from its primary site, the overall survival rate is very poor and there is no surgical resection option available for treatment. There are many chemotherapeutic strategies, but the long-term benefits have little chances of success due to drug resistance, that often occurs. Based on this evidence, finding new possible therapeutic targets represents a real urgency for this type of aggressive and lethal tumor.

Melanoma microenvironment is characterized by low O_2 levels, which trigger the expression of CAXII. This metalloenzyme is responsible for TME acidification, along with cancer migration and invasion. For this reason, CAXII has been investigated as both therapeutic target and prognostic marker for many cancers, but no evidence regards melanoma. Moreover, aberrant re-activation of the Hh pathway is also associated to melanoma migration and emerging evidence suggest that the Hh cascade may represent a promising therapeutic target. A recent study observed a correlation between the Hh and CAXII in breast cancer [125] but in melanoma they have not been correlated before. For all these reasons, the aims of this thesis are:

- investigating if a correlation between the Hh and CAXII occurs in melanoma;
- determining the role of the Hh and CAXII in melanoma migration and invasion;
- examining CAXII as possible therapeutic target, performing two different inhibitory strategies.

3. MATERIAL AND METHODS

3.1 Cell cultures

SK-MEL-28 and A375 were kindly provided by Dr. Francesca Chiarini (CNR Institute of Molecular Genetics "Luigi Luca Cavalli-Sforza", Bologna, Italy) and Prof. Luisa Bracci (Department of Medical Biotechnologies, University of Siena) respectively. SK-MEL-28 were maintained in RPMI 1640, whereas Dulbecco's modified Eagle's medium (DMEM) was used for A375 (both Euroclone, Devon, UK). Media were supplemented with antibiotics (100 U/ml), L-glutamin (2 mM) and 10% fetal bovine serum (FBS, Euroclone, Devon, UK) and incubated in humidified atmosphere with 5% CO_2.

3.2 Hypoxic treatment

Hypoxic experiments were conducted using the InVivo 400 workstation (Ruskinn, Pencoed, UK) or hypoxic incubator $CO_2/O_2/N_2$ (Sanyo, Moriguchi, Japan). Both provided a humidified and stable microenvironment set at 5% CO_2, 2%O_2 (corresponding to pO_2 ~ 14 mmHg) and 37°C temperature. The pO_2 was constantly regulated and maintained with the addition of N_2.

Figure 16: the hypoxic InVivo 400 workstation (Ruskinn, Pencoed, UK).

3.3 Transient transfection

SMO and CTR small interfering RNA (siRNAs) (Sigma-Aldrich, Saint Louis, MO, USA), and GLI1 and CAXII siRNAs (Invitrogen, Paisley, UK) were resuspended in DNAase and RNAase free water (Sigma-Aldrich, Saint Louis, MO, USA) and used at a final concentration of 100 nM. Two different sirnas for each target were tested and the one which got the best silencing results for the cells was used. Transfections were achieved using Neon™ transfection system (Invitrogen, Paisley, UK). Cells were seeded at different density according to experiment: 5 x 10^5 cells per 35 x 10 mm culture dish for western blot, 3.5 x 10^5 cells/well per 24-well plate for RT-qPCR, 2 x 10^4 cells per side of insert for scratch assay and invasion assays and 1 x 10^4 cells/well per 96-well for spheroid formation. For transfection experiments, RPMI or DMEM supplemented with L-glut and 10% FBS but without antibiotics were required.

3.4 Chemical compounds

3.4.1 Glabrescione B

Glabrescione B (GlaB) is the first small molecule designed to bind GLI1 zinc finger, with consequent impairment of its interaction with DNA [126]. GlaB was diluted in dimethyl sulfoxide (DMSO) and used at a final concentration of 1 µM.

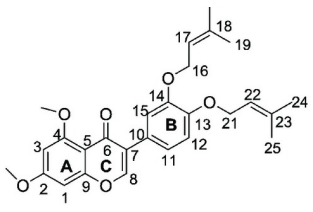

Figure 17: GlaB chemical structure (modified from Infante et al., [126]).

3.4.2 Compound 22

Compound 22 (C22) is a multitarget compound that acts both on SMO and GLI1 suppressing the Hh pathway at upstream and downstream level [127]. The inhibitor was resuspended in DMSO and used at a final concentration of 1 µM.

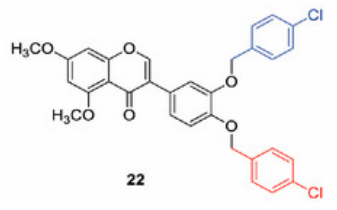

Figure 18: C22 chemical structure (modified from Lospinoso et al., [127]).

3.4.3 GV2-20

GV2-20 is a benzoic acid derivate previously identified as CAs inhibitor by a computation-driven target [128]. I here used it as a pan-CAs inhibitor. It was resuspended in DMSO and used at a final concentration of 10 nM.

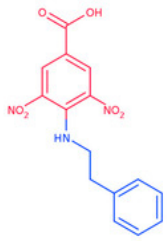

Figure 19: GV2-20 chemical structure (modified from Mori et al., [128]).

3.4.4 Compound 7-10

Considering the nature and the efficacy of GV2-20, 17 chemically different compounds bearing the 3-nitrobenzoic acid substructure were synthesized. After testing all compounds for their inhibitory activity against pharmacologically relevant CAs isoforms, compounds 7 (C-7) was identified as the most selective against CAIX, whereas compound 10 (C-10) resulted the
most selective against both CAIX and CAXII (**figure 20**) [129]. Both the inhibitors were resuspended in DMSO and used at a final concentration of 10 nM.

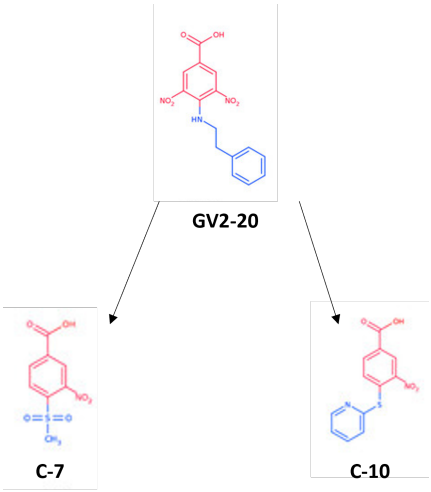

Figure 20: C-7 and C-10 chemical structures (modified from Cau et al., [129]).

3.4.5 Acetazolamide

Acetazolamide (AAZ) is a sulfonamide derivative and it was used as reference compound among CAs inhibitors. It was diluted in DMSO and used at a final concentration of 10 nM.

3.4.6 Ara-C

Due to its ability to incorporate into DNA and inhibits replication, cytosine β-D-arabinofuranoside Ara-C (Sigma Aldrich, Saint Louis, MO, USA) was used as antiproliferative molecule during migration assays at a concentration of 2.5 µg/ml.

3.5 Cell viability

SK-MEL-28 and A375 were seeded in 96-well plates (Corning, New York, NY, USA) at a density of 2 x 10^4 cells in 50 µl/well and treated with CAs inhibitors for 72h. Then, cell viability was detected using fluorescein diacetate (1 mg/ml, dilution 1:200) and viability index was calculated as the percentage of the ratio between treated groups and control (CTR). The experiments ware conducted under both normoxia and hypoxia and repeated at least three times.

3.6 Western blot

Cells were seeded in 60 mm petri dishes (Corning, New York, NY, USA) at a density of 4 x 10^5 for SK-MEL-28 and 6 x 10^5 for A375 and, following with specific treatments, incubated for 24 h or 48 h under normoxic or hypoxic condition. Thereafter, cells were washed with cold PBS without CA^{2+}

and Mg^{2+} and were lysed with 40 µl Laemmli buffer 2X supplemented with a cocktail of proteinase inhibitors (Sigma Aldrich, Saint Louis, MO, USA). After sonication and quantification of the total protein amount using Micro BCA Protein Assay Reagent kit (Thermo Fisher Scientific, Cleveland, OH, USA), 30 µg per lane were loaded onto SDS-PAGE gels at 8-10% acrylamide (Sigma Aldrich, Saint Louis, MO, USA) and blotted onto nitrocellulose membranes 0.2 µm (BIO-RAD, Hercules, CA, USA). Non-specific protein binding sites were saturated incubating membranes with 5% nonfat powder milk for 1 h at room temperature and three washing with TBST 1% Tween (Sigma Aldrich, Saint Louis, MO, USA) were followed. Thereafter, membranes were incubated overnight at + 4° C with primary antibodies listed below (**table 2**).

Primary antibody	Dilution	Purchased from
Anti-HIF-1α	1.500	BD
Anti-SMO	1:500	Santa Cruz, Santa Cruz, CA, USA
Anti-GLI1	1:1000	Cell signaling, Denver, CO, USA
Anti-CAXII	1:500	Santa Cruz, Santa Cruz, CA, USA
Anti-phFAK	1:1000	Cell signaling, Denver, CO, USA
Anti-FAK	1:1000	Cell signaling, Denver, CO, USA
Anti-β-Actin	1:50000	Sigma Aldrich, Saint Louis, MO, USA

Table 2: List of primary antibodies for immunoblotting.

The following day, specific anti-mouse IgG HRP and anti-rabbit IgG-HRP (Cell Signaling Technologies, Danvers, MA, USA) secondary antibodies were used. Following chemiluminescence detection of the immunoreactive bands using ChemiDoc™ MP System (Bio-Rad, Hercules, CA, USA), analyses of quantification were conducted via Image Lab software (Bio-Rad Laboratories, Hercules, CA, USA).

3.7 RNA extraction and RT-qPCR

Cells were seeded in 6-well plates (Corning, New York, NY, USA) at a density of 3.5 x 10^5 cells for SK-MEL-28 and 4.5 x 10^5 for A375 and incubated under both normoxia and hypoxia. At the time of 24 h or 48 h of specific treatments, cells were isolated with EuroGOLD™Trifast reagent (Euroclone, Devon, UK) and the addition of chloroform and the centrifugation at 14 000 x g triggered the separation of the sample into three phases: an organic phase on the bottom of the tube

containing proteins and cellular debris, an intermediate opaque phase containing DNA and an aqueous upper phase containing the total RNA. The aqueous RNA was transferred into a new tube and then washed firstly with isopropanol and then with cold 75% ethanol. Thereafter, extracted RNA was suspended in nuclease free water, boiled 10 minutes at 56°C and stored at -80°C for short time. RNA quantification was evaluated with the Thermo Scientific™ NanoDrop™ One Microvolume UV-Vis Spectrophotometer (Thermo Fisher, Thermo Fisher Scientific, Waltham, MA, USA).

Complementary DNA (cDNA) was synthetized using iScript™cDNA Synthesis Kit (Bio-Rad Laboratories, Hercules, CA, USA) and reverse transcription quantitative polymerase chain reaction (RT-qPCR) was performed with SsoAdvanced™ Universal SYBR® Green Supermix (Bio-Rad Laboratories, Hercules, CA, USA). mRNA levels were determined by MiniOPTICON™ System (Bio-Rad Laboratories, Hercules, CA, USA) and quantitative analyses were conducted by iQ5™ Optical System Software (Bio-Rad Laboratories, Hercules, CA, USA). The relative quantification was calculated using $2^{-\Delta\Delta CT}$ method [130] and L32 was used as housekeeping gene. Validated GLI1 and L32 primers were purchased from Invitrogen (Thermo Fisher Scientific, Cleveland, OH, USA), whereas SMO and CAXII from Sigma Aldrich (Saint Louis, MO, USA) (**table 3**).

Gene	Forward	Reverse
GLI1	5' TTCCTACCAGAGTCCCAAGT	5' CCCTATGTCAAGCCCTATTT
SMO	5' CTTTGTCATCGTGTACTACGCC	5' CGAGAGAGGCTGGTAGGTC
CAXII	5' CTGGCATCATGTATTTAGGGGC	5' GAGTTGCGCCTGTCAGAAAC
L32	5' GCTGGAAGTGCTGCTGATGTG	5' CGATGGCTTTGCGGTTCTTGG

Table 3: List of primer pair sequences.

3.8 Scratch assay

SK-MEL-28 and A375 were transfected with 100 nM specific siRNAs and thereafter were seeded in culture-insert 2 well in µ-Dish 35 mm (Ibidi, Munich, Germany). In each insert 2 x 10^4 cells for SK-MEL-28 and 3 x 10^4 for A375 were seeded. The experiment was conducted both in normoxia and hypoxia. After allowing cells to attach overnight, the silicone inserts were removed to create a cell-free gap of approximately 500 µm and refresh medium supplemented with Ara-C 2.5 µg/ml was added. Migration ability was monitored and snapshots of the scratch were taken at time 0, 24 and 48 h with an inverted microscope (Olympus IX81, Tokyo, Japan) at 10 x magnification. The wound

measures were quantified using ImageJ software. Data were reported as $\left(1-\frac{Ax}{A0}\right)$%, where A0 and Ax represented the empty area at time 0 and 24 or 48 h.

For chemical compounds, cells were pretreated overnight with specific inhibitors and fresh medium supplemented with new treatments were added after removed silicon insert.

3.9 Modified Boyden chamber

Invasion assay was performed using Boyden 48-well micro chemotaxis Chambers (Neuro Probe, Gaithersburg, MD, UK) with 8µm pore size polycarbonate polyvinylpyrrolidone-free nucleopore filters, as already described by Albini et al., [131, 132]. The filters were previously precoated with 100 µl of 0.2 mg/ml Matrigel (Corning, Life Science, Corning, Tewksbury, MA, USA).
40'000 of transfected cells or 25'000 pretreated cells were plated in 50 µl of RPMI or DMEM with 0.1 % BSA, without FBS, supplemented with 1µM of specific compound when required. NIH3T3 supernatant was used as chemoattractant in the lower chamber compartment. After 24 h experiment, cells were fixed and stained with Diff Quick (Merz-Dade, Düdingen, Switzerland) and photographed at 5 X with an OLYMPUS IX81 inverted microscope. Invaded cells in four high-power field were counted and data were expressed as number of invaded cells/field.

3.10 Zymography

To detect the enzymatic activity of cells secreted MMP-9, I performed a zymogram assay. The activity is measured evaluating the ability of MMP-9 to digest the substrate (in this specific case gelatin from porcine skin, (Sigma Aldrich, Saint Louis, MO, USA)). Media from 24 h experiments conducted both under normoxic or hypoxic condition were collected, centrifuged at 300 x g for 5 minutes to remove cell debris, and quantified using Micro BCA Protein Assay Reagent kit (Thermo Fisher Scientific, Cleveland, OH, USA). 10 µg of each diluted media was load onto 10% resolving gel with 30%acrylamide/0.8%bisacrylamide, 1.5M Tris-Hcl pH 8.8, 1% Gelatin (Type A, from Porcine skin, Sigma Aldrich) (20mg/ml), APS and TEMED in ddH2O and a 4% stacking gel containing 30%acrylamide/0.8%bisacrylamide, 0.5 M Tris-HCl pH 6.8, SDS, APS and TEMED in ddH2O. After running for 90 minutes at a 125V, the gel was then incubated in developing buffer in agitation at 37° C overnight, to reproduce a favorable microenvironment for MMPs activity. The day after, gels

were stained with Comassie R-250 (Sigma Aldrich, Saint Louis, MO, USA), pictures were taken with ChemiDoc™ MP System (Bio-Rad, Hercules, CA, USA) and quantified using ImageJ software.

3.11 Spheroids

6'000 cells for SK-MEL-28 and 10'000 cells for A375 were seeded in PrimeSurface® 96U plate (Twin Helix, Milan, Italy) in 50 µl and treated with 1 µM of specific inhibitors. Fresh treatments were added three times a week. Images were taken every day for 20 days with inverted microscope Olympus IX81 at 10 X magnification.

3.12 Statistical analyses

Data are presented as mean and ± SEM of at least three independent experiments, performed in duplicates or triplicates. Statistical analyses were conducted using unpaired *t*-test and analysis of variance (ANOVA) with Graph-pad Prism 7 software (San Diego, CA, USA). Statistical significance was set at $P \leq 0.05$ (* $P \leq 0.05$, ** $P \leq 0.01$).

4. RESULTS

4.1 SMO and GLI1 transient silencing affected CAXII protein expression

In order to mimic the TME pO_2, experiments were conducted both under normoxic and hypoxic condition. For this reason, as first I verified HIF-1α expression in SK-MEL-28 and A375 after 24 h incubation. As **figure 21 A** shows, both cell lines expressed significantly higher protein levels of HIF-1α under hypoxia compared to normoxia. These results confirmed that the pO_2 employed in the experiments was adequate to induce hypoxic state.

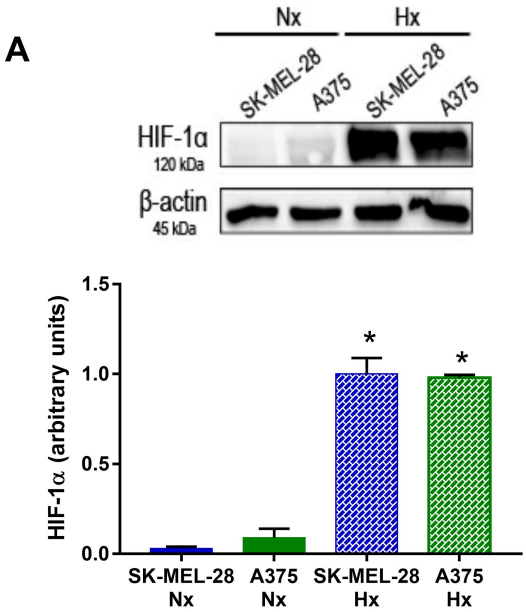

Figure 21: A) HIF-1α protein expression after 24 h incubation either under normoxic or hypoxic condition in SK-MEL-28 and A375. B-actin was used as loading control for Western Blot and L32 as housekeeping gene for RT-qPCR. Blots are representative images and data are presented as the mean and ± SEM of three independent experiments. * $p \leq 0.05$ indicates statistically significant differences.

After that, I performed SMO and GLI1 transient transfection via siRNA technology. Control (CTR) cells transfected with non-targeting oligos were used as negative control. As **figure 21 B-C** report, SMO mRNA and protein levels were significantly reduced after 24 h transfection with SMO siRNA in SK-MEL-28, both under normoxic and hypoxic condition. Similar results were obtained also in A375 after 48 h transfection (**figure 21 D-E**).

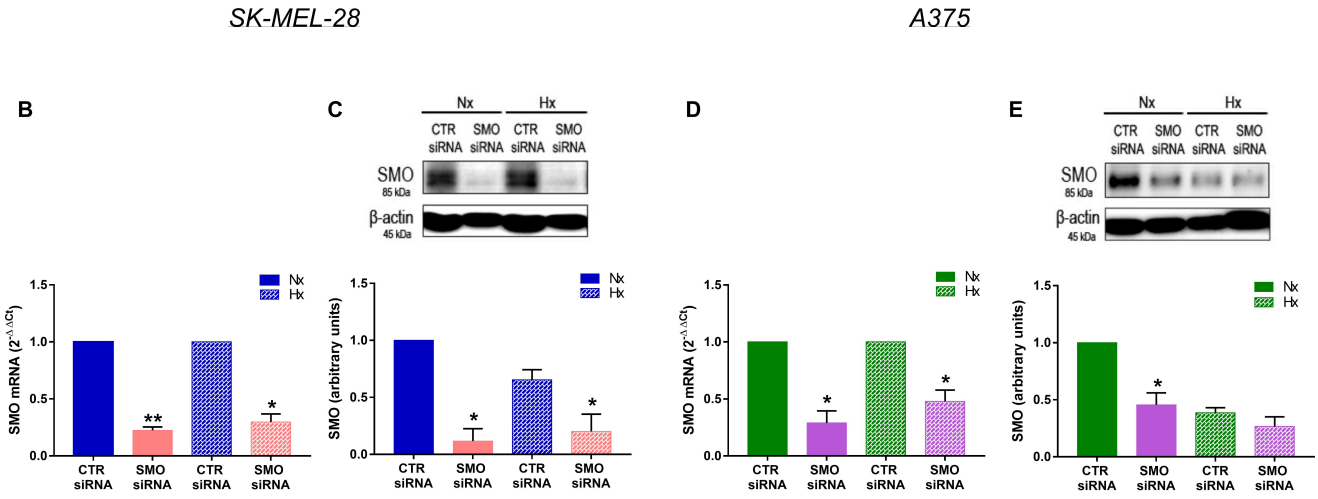

Figure 21: B) Smoothened (SMO) RT-qPCR and **C**) Western Blot analyses after 24 h silencing with SMO small interfering RNA (siRNA) under normoxic or hypoxic condition in SK-MEL-28 cell line; **D**) SMO RT-qPCR and **E**) Western Blot analyses after 48 h silencing with SMO siRNA under normoxic or hypoxic condition in A375 cell line. B-actin was used as loading control for Western Blot and L32 as housekeeping gene for RT-qPCR. Blots are representative images and data are presented as the mean and ± SEM of three independent experiments. * $p \leq 0.05$ and ** $p \leq 0.01$ indicate statistically significant differences.

Moreover, GLI1 transfection also reported good results, as GLI1 mRNA and protein levels resulted to be significantly decreased in SK-MEL-28 after 24 h silencing and this occurred both under normoxia and hypoxia (**figure 21 F-G**). Eventually, A375 cells were also effective to GLI1 knock down after 48 h transfection, as RT-qPCR and western blot analyses show in **figure 21 H-I**. Of interest to note that in addition to the effectiveness of our method of silencing, also the hypoxic condition decreases the activity of the Hh pathway. Thus, hypoxic SMO and GLI1 protein controls resulted decreased compared to the normoxic ones and this phenomenon occurred both in SK-MEL-28 and A375.

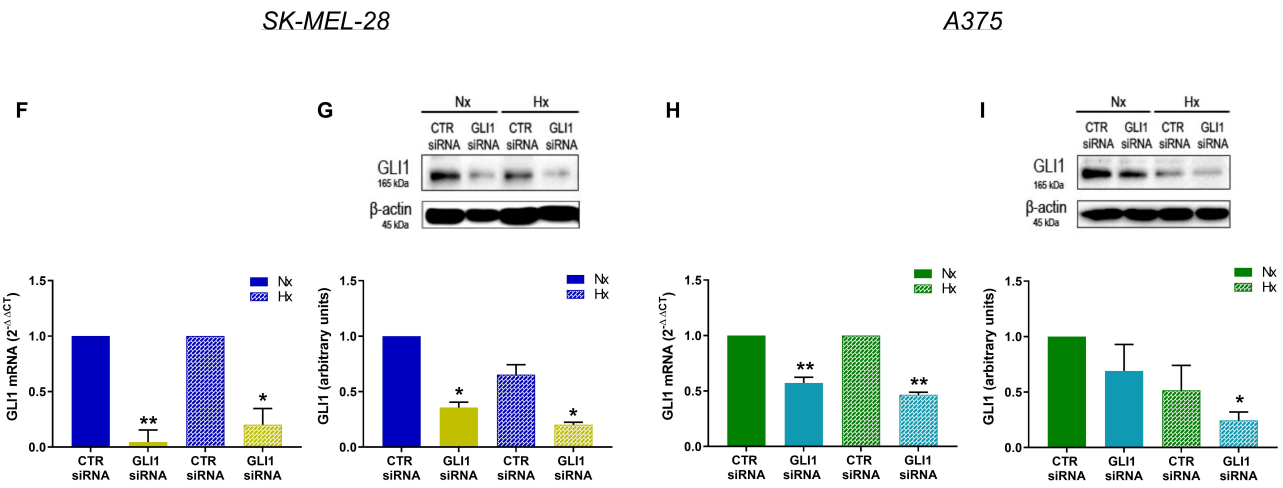

Figure 21: F) GLI1 RT-qPCR and **G**) Western Blot analyses after 24 h silencing with GLI1 siRNA under normoxic or hypoxic condition in SK-MEL-28 cell line; **H**) GLI1 RT-qPCR and **I**) Western Blot analyses after 48 h silencing with GLI1 siRNA under normoxic or hypoxic condition in A375 cell line. B-actin was used as loading control for Western Blot and L32 as housekeeping gene for RT-qPCR. Blots are representative image and data are presented as the mean and ± SEM of three independent experiments. * $p \leq 0.05$ and ** $p \leq 0.01$ indicate statistically significant differences.

Defined the efficacy of the biological silencing here used, I next evaluated the effect of the Hh knock down on CAXII protein expression. The Hh pathway and CAs have been already investigated in melanoma but they have not been correlated before, reason why I tried to understand if the Hh pathway may be involved in CAs modulation. Hence, I used both SMO and GLI1 transfection to examine whether the Hh cascade could interfere with CAXII expression and if the potentially interaction may be SMO- or GLI1-dependent. From **figure 22 A-B** emerge that SMO siRNA significantly decreased CAXII levels both under normoxic and much more under hypoxic conditions in both cell lines. Conversely, GLI1 knock down was not significantly effective on CAXII protein levels under normoxia, both in SK-MEL-28 and A375 cell lines, whereas such silencing resulted to be strongly effective under hypoxia, where CAXII control groups were upregulated (**figure 22 C-D**).

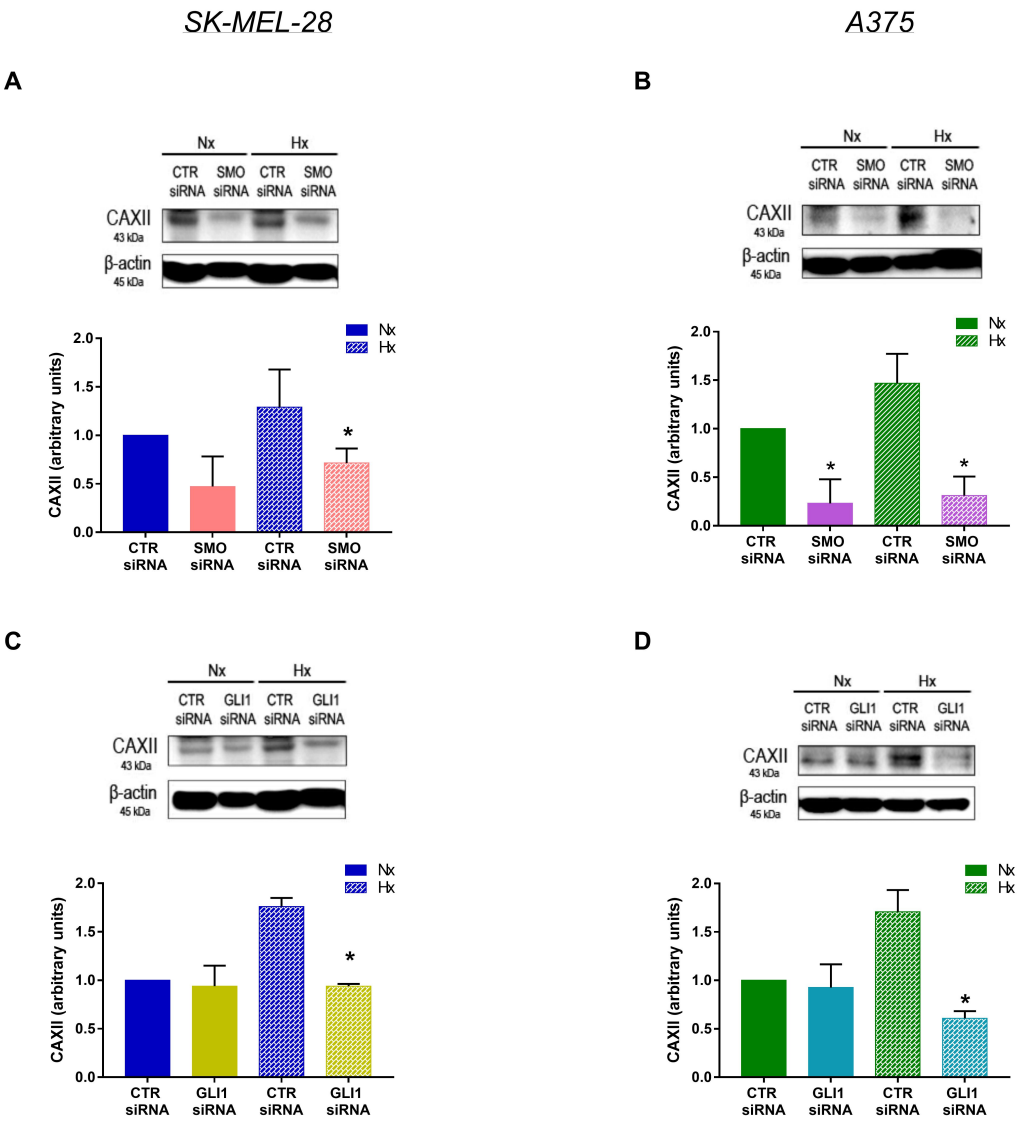

Figure 22: A) Carbonic Anhydrase XII (CAXII) protein expression after 24 h transfection with SMO siRNA under normoxia or hypoxia in SK-MEL-28 and **B**) after 48 h in A375; **C**) CAXII protein expression after 24 h transfection with GLI1 siRNA under normoxia or hypoxia in SK-MEL-28 and **D**) after 48 h in A375. B-actin was used as loading control, the blots report representative images and data are presented as the mean and ± SEM of three independent experiments. * $p \leq 0.05$ indicates statistically significant differences.

4.2 SMO and GLI1 knock down impaired melanoma migration and invasion

Established the effects of SMO and GLI1 knock down on CAXII expression, I investigated the functional impact of such silencing on cell migration and invasion ability. With the aim to deep understand the spreading mechanism, I here used two difference grade of malignant melanoma cells: the intermediate metastatic SK-MEL-28 and the highly metastatic A375 [133]. To this purpose, after transfection I performed scratch assays and monitored cell ability to repair the gaps up to 48 h. **Figure 23 A** shows that the Hh knock down significantly damaged SK-MEL-28 migration as of 24 h under normoxia, with major effects reported by SMO silencing, due to which cells migrated just 20%. However, the most severe effects were seen under hypoxia, where control group was completely repaired after 48 h experiment, whereas SMO and GLI1 siRNAs repaired just for 40% and 60% the empty area respectively. Moreover, a similar trend was also obtained in A375 (**figure 23 B**), where both SMO and GLI1 silencing strongly impaired migration ability, both under normoxia and hypoxia, without differences between SMO or GLI1 siRNA treatment.

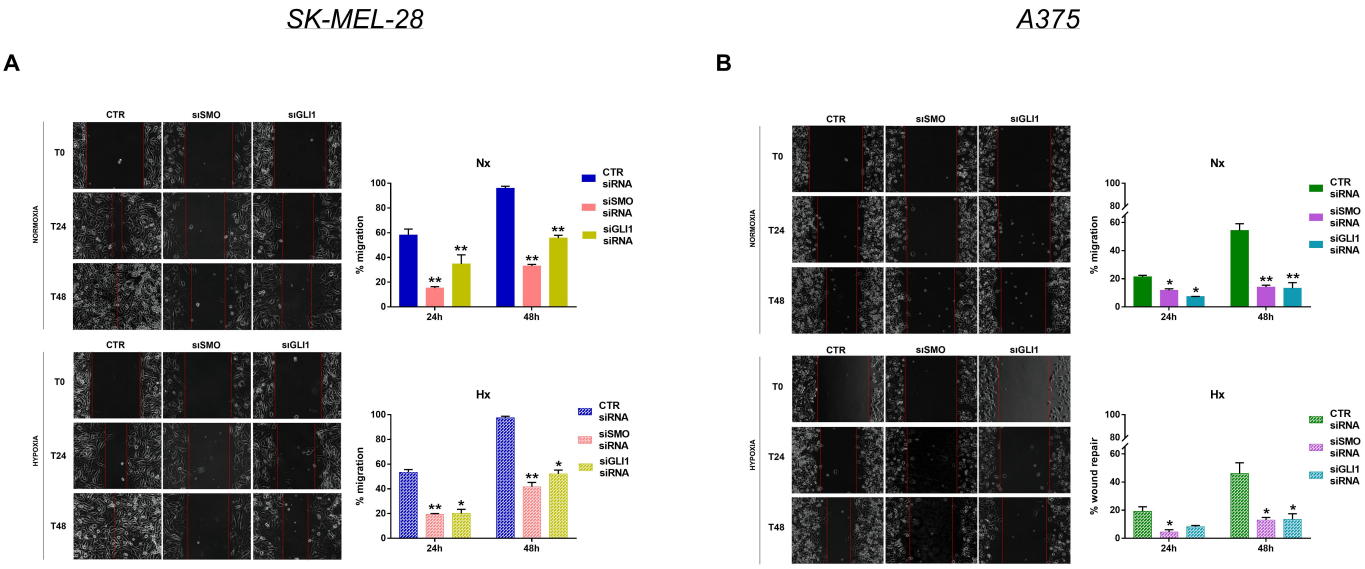

Figure 24: Wound healing assays performed with SMO and GLI1 siRNAs at 24 h and 48 h under normoxic or hypoxic condition in SK-MEL-28 (**A**) and A375 (**B**); Reported pictures are representative and data are reported as the mean and ± SEM of three independent experiments. * $p \leq 0.05$ and ** $p \leq 0.01$ indicate statistically significant differences.

One of the major features of malignant cells is the ability to create space between barriers to enter the blood or lymphatic circulation and disseminate as metastasis. To this aim, I performed a modified Boyden chamber assay to assess the impact of the Hh inhibition in melanoma invasion.

As **figure 24 C** demonstrates, SK-MEL-28 invasion was strongly reduced with SMO and GLI1 siRNAs after 24 h experiment both in normoxia and much more in hypoxia, where SMO silencing seems to be much more effective than GLI1 siRNA. On the contrary, the Hh inhibition had little effects on A375 invasion capacity under normoxia, while by both SMO and GLI1 treatments a significant reduction was obtained under hypoxia, where metastatic melanoma is facilitated to spread (**figure 24 D**). It is interesting to note how hypoxia affected invasive capacity differently between the two types of melanomas: while hypoxia played a fundamental role in stimulating highly metastatic A375 invasion, there was no difference in infiltration between normoxic and hypoxic controls for the intermediate metastatic SK-MEL-28.

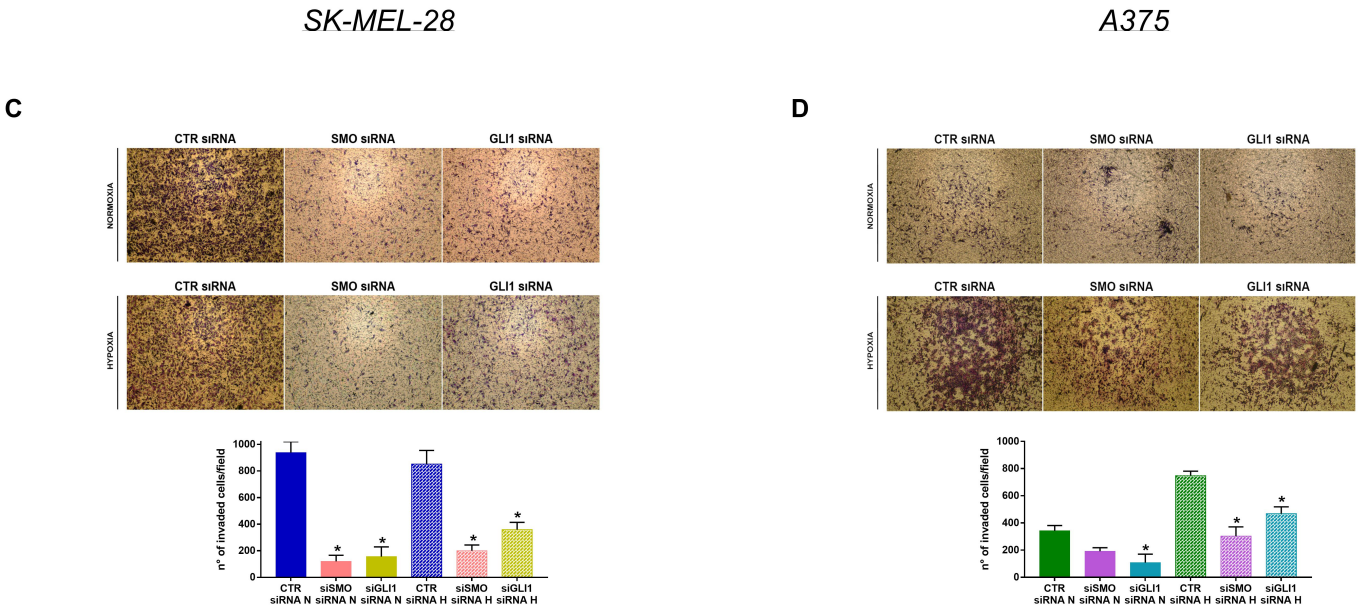

Figure 24: modified Boyden chamber with SMO and GLI1 siRNAs after 24 h under normoxic or hypoxic condition in SK-MEL-28 (**C**) and A375 (**D**). Reported pictures are representative and data are reported as the mean and ± SEM of three independent experiments. * $p \leq 0.05$ indicates statistically significant differences.

4.3 CAXII silencing also impaired melanoma migration and invasion

Since the correlation between the Hh pathway and CAXII has been here observed, I tried to elucidate whether the molecular mechanism that correlates the Hh pathway inhibition with reduced melanoma dissemination, could be connected to CAXII activity. For this reason, a CAXII silencing via siRNA technology was performed and again the impact of such inhibition in terms of migration and invasion was evaluated. As first, we attested the efficacy of such silencing on mRNA and protein expression in both cell lines. As **figure 25 A** shows, CAXII-targeted siRNA resulted in significant decreased CAXII mRNA levels after 24 h treatment under hypoxia in SK-MEL-28 and this was confirmed also by Western blot analysis (**figure 25 B**). However, CAXII silencing was more effective in A375, where both CAXII mRNA and protein levels resulted significantly impaired after 48 h experiment (**figure 25 C-D**).

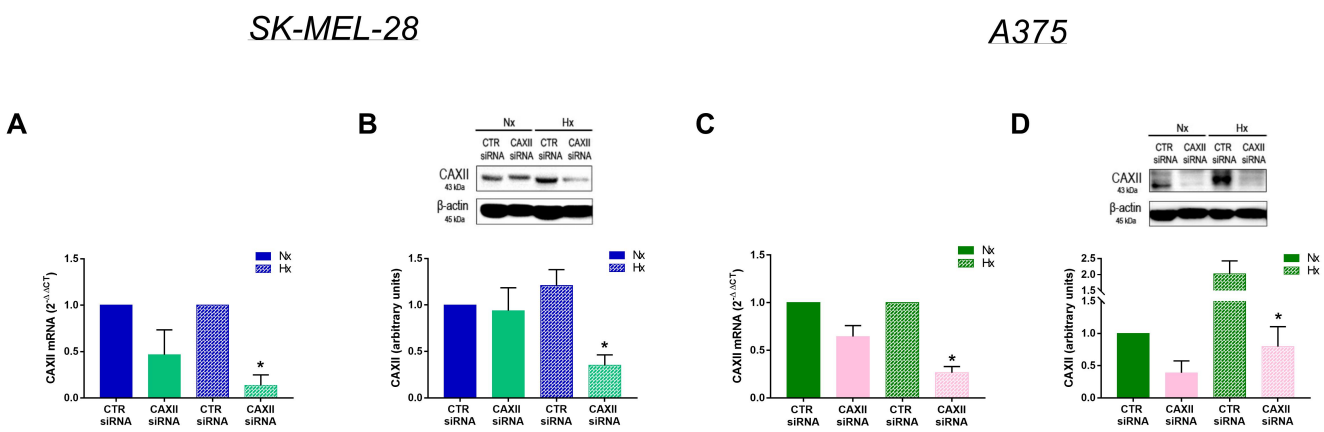

Figure 25: CAXII RT-qPCR (**A**) and Western Blot analyses (**B**) after 24 h silencing with CAXII siRNA under normoxic or hypoxic condition in SK-MEL-28; CAXII RT-qPCR (**C**) and Western Blot analyses (**D**) after 48 h silencing with CAXII siRNA under normoxic or hypoxic condition in A375. B-actin was used as loading control for Western Blot and L32 was used as housekeeping gene for RT-qPCR. Reported blots and pictures are representative and data are presented as the mean and ± SEM of three independent experiments. * $p \leq 0.05$ indicates statistically significant differences.

Thereafter, evaluation of migration ability after CAXII-targeted siRNA treatment was followed. **Figure 25 E** reports that CAXII-silenced SK-MEL-28 were not able to repair the scratch 48 h after transfection, both under normoxic and hypoxic condition, whereas control siRNAs completely closed the wounds. Similar trends were registered also by A375 (**figure 25 F**), where the effects of CAXII knock down were significantly evident, despite a slower migration compared to SK-MEL-28 cells.

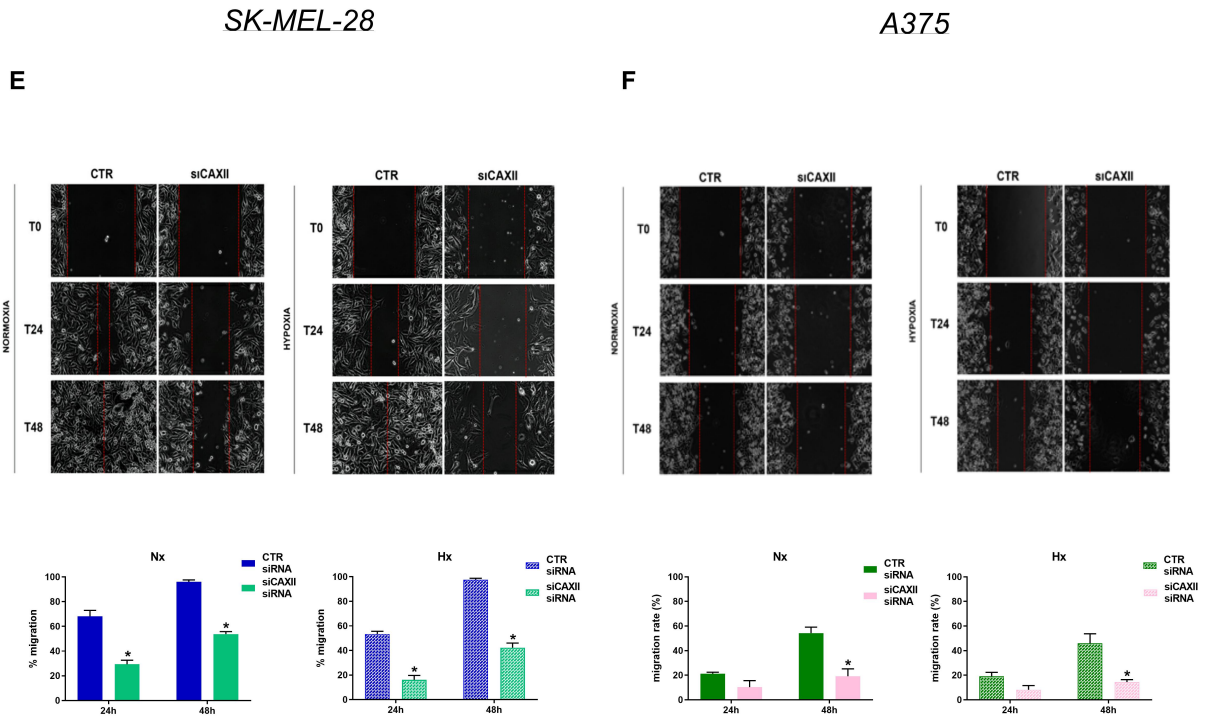

Figure 25: Wound healing assays performed with CAXII siRNA at 24 h and 48 h under normoxic or hypoxic condition in SK-MEL-28 (**E**) and A375 (**F**). Reported pictures are representative and data are presented as the mean and ± SEM of three independent experiments. * $p \leq 0.05$ indicates statistically significant differences.

Lastly, CAXII suppression was verified also in term of invasiveness. In accordance with the migration results above, CAXII knock down significantly inhibited SK-MEL-28 invading ability both under normoxia and hypoxia (**figure 25 G**), whereas such silencing resulted significantly effective only in hypoxia for A375 (**figure 25 H**). Even in this case, we observed the hypoxic influence on A375 invasiveness.

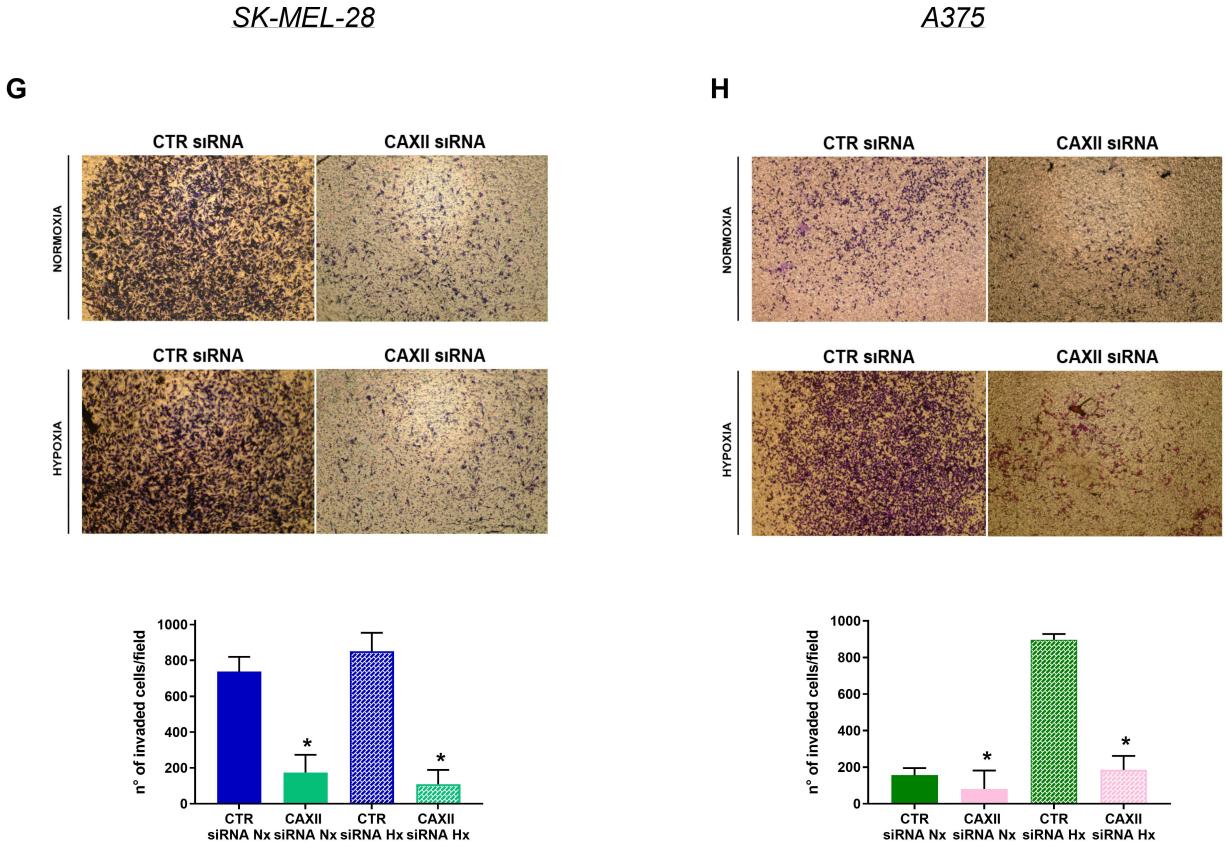

Figure 25: modified Boyden chamber with CAXII siRNA after 24 h under normoxic or hypoxic condition in SK-MEL-28 (**G**) and A375 (**H**). B-actin was used as loading control for Western Blot and L32 was used as housekeeping gene for RT-qPCR. Reported blots and pictures are representative and data are presented as the mean and ± SEM of three independent experiments. * $p \leq 0.05$ indicates statistically significant differences.

4.4 Glabrescione B and Compound 22 as newly compound targeting the Hh pathway

Since the biological suppression of the Hh pathway reported promising results, I tried to use new designed small molecules and investigated if the same inhibitory effects could be obtained also by chemical treatment. In this regard, it is reported that small molecules are important tools to target pathways involved in tumorigenesis or cancer progression and in the field of the Hh pathway, many efforts have been made to improve their availability; nevertheless, target mutations or drug resistance have risen the exigency of new therapeutic strategies. In light of this evidence, I here tested the biological efficacy of two new small chemical inhibitors: GlaB and C22 (described in the material and method section) [126, 127]. As first, I verified the suppressive efficacy of the two compounds on SMO and GLI1 protein expression after 24 h treatment, under both normoxic and hypoxic condition. Western blot analyses reported in **figure 26 A** confirmed the efficacy of the multitarget C22 on SMO expression, in a same trend under normoxic or hypoxic condition for SK-MEL-28. C22 was also effective on GLI1 protein expression both under normoxia and hypoxia (**figure 26 C**). Not only that, hypoxic GLI1 levels of SK-MEL-28 were also sensitive to GlaB treatment, as **figure 26 C** shows.

In A375 cell line, C22 treatment significantly impaired SMO protein expression under hypoxia (**figure 26 B**), whereas GLI1 was strongly reduced under both normoxia and hypoxia (**figure 26 D**). Eventually, hypoxic GLI1 protein expression was also significantly affected by GlaB treatment (**figure 26 D**).

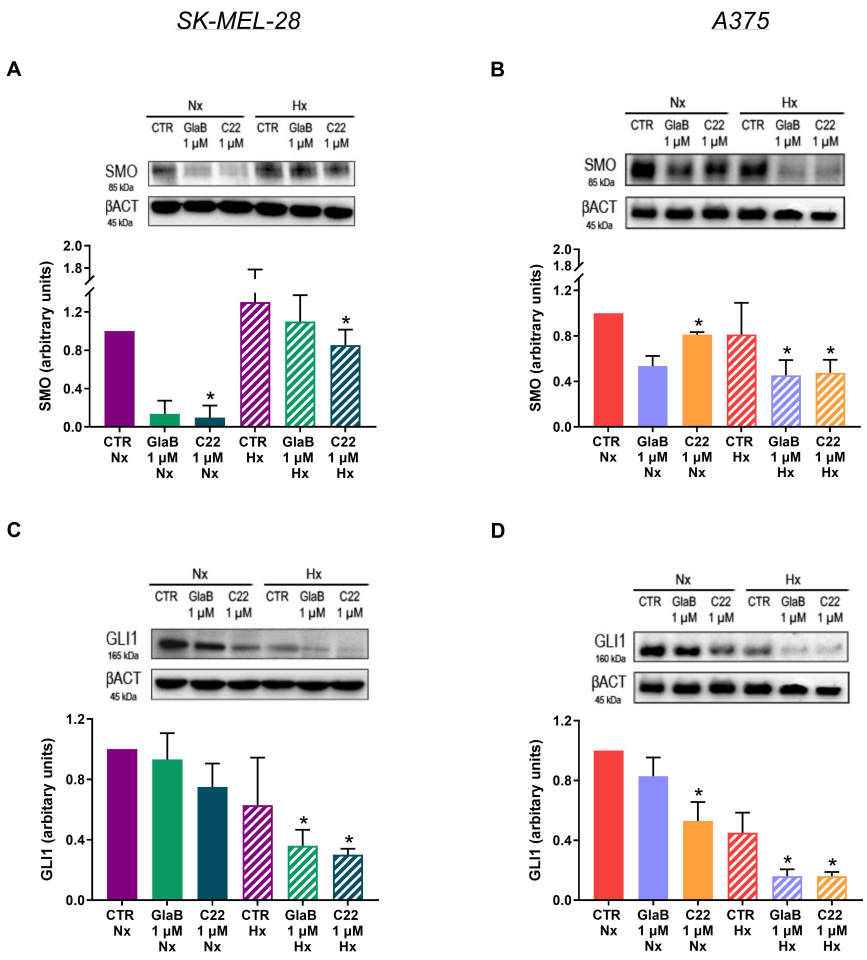

Figure 26: SMO protein expressions after 24 h treatment with Glabrescione B (GlaB) 1µM and compound 22 (C22) 1µM under normoxic and hypoxic condition in SK-MEL-28 (**A**) and A375 (**B**); GLI1 protein expressions after 24 h treatment with GlaB 1µM and C22 1µM under normoxic and hypoxic condition in SK-MEL-28 (**C**) and A375 (**D**). B-actin was used as loading control, all blots report a representative image and data are presented as the mean and ± SEM of three independent experiments. * $p \leq 0.05$ indicates statistically significant differences.

Thereafter, I investigated if CAXII inhibition via suppression of the Hh pathway occured even by chemical treatment. At this purpose, western blot analyses after 24 h treatment with GlaB and C22 were performed. As **figure 26 E** displays, both GlaB and C22 treatment significantly decreased CAXII expression in SK-MEL-28, under both normoxia and hypoxia. Similarly, CAXII protein expression was significantly impaired by C22 also in A375 (**figure 26 F**), but the major effects are reported by GlaB treatment, with similar trend in normoxia and hypoxia.

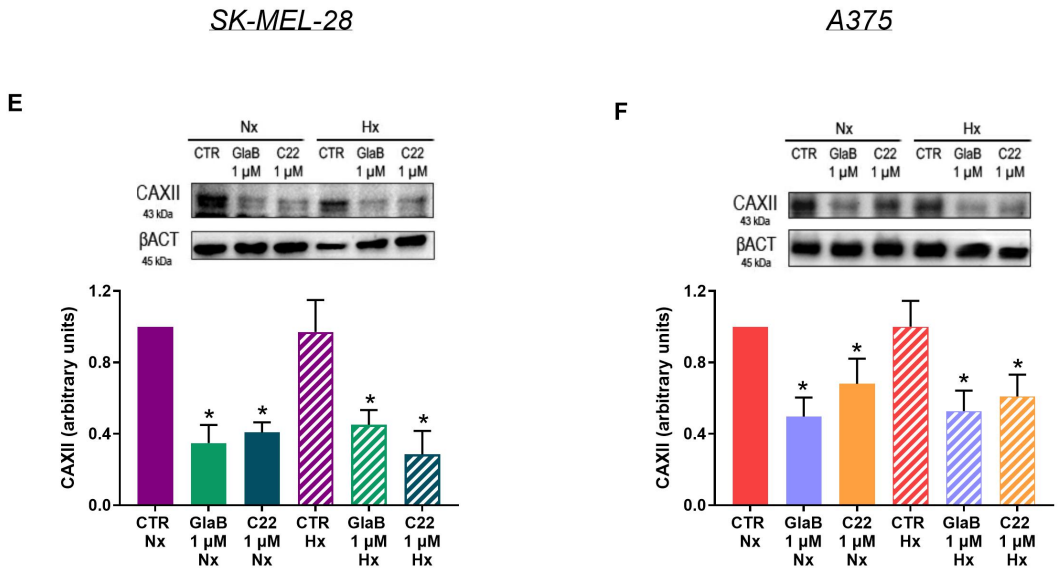

Figure 26: CAXII protein expressions after 24 h treatment with GlaB 1µM and C22 1µM under normoxic and hypoxic condition in SK-MEL-28 (**E**) and A375 (**F**). B-actin was used as loading control, all blots report a representative image and data are presented as the mean and ± SEM of three independent experiments. * $p \leq 0.05$ indicates statistically significant differences.

4.5 GlaB and C22 impaired melanoma cell migration and invasion

At this point, GlaB and C22 were tested as possible therapeutic molecules to fight malignant melanoma dissemination. To this purpose, scratch assays were repeated in both cell lines and the experiments were conducted both in normoxia and hypoxia. As **figure 27 A** shows, GlaB and C22 significantly decreased SK-MEL-28 migration at 24 h treatment, under both normoxia and hypoxia, and the effects were enhanced at 48 h, when CTR cells completely repaired. Of interest, C22 treatment resulted to be more efficient, as normoxic and hypoxic SK-MEL-28 seem not be able to repair over 30% of the gaps. Similarly, both SMO and GLI1 inhibitors markedly damaged A375

migration, with almost no differences within treatments and normoxic hypoxic condition (**figure 27 B**).

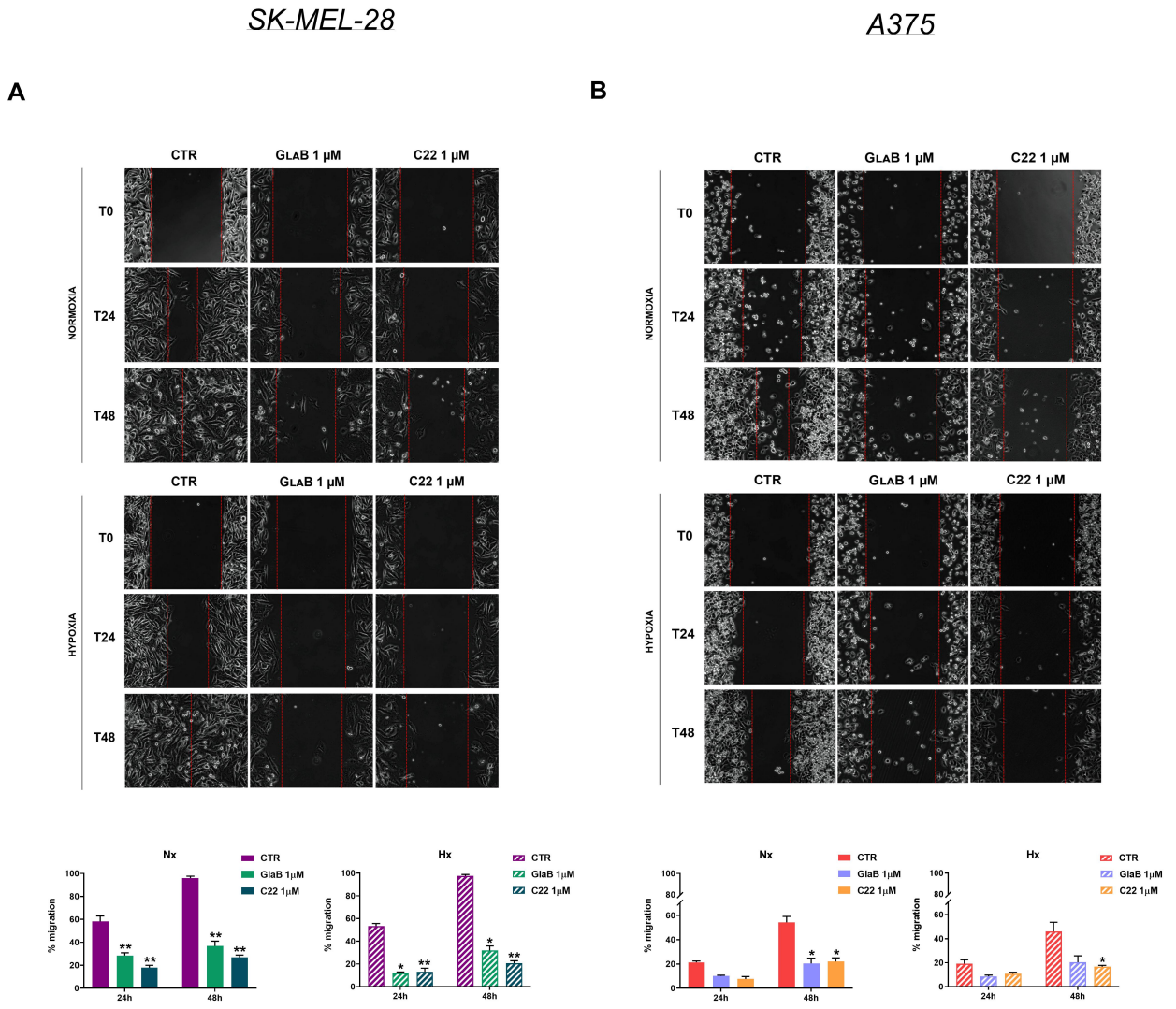

Figure 27: scratch assays performed with GlaB 1µM and C22 1µM treatments at 24 h and 48 h under normoxic or hypoxic condition in SK-MEL-28 (**A**) and A375 (**B**); Reported pictures are representative and data are presented as the mean and ± SEM of three independent experiments. * $p \leq 0.05$ and ** $p \leq 0.01$ indicate statistically significant differences.

Furthermore, again SK-MEL-28 and A375 invasion ability was tested and even in this case the effects of the Hh inhibition were still visible; indeed, inhibition of GLI1 activity by GlaB treatment affected both SK-MEL-28 (**figure 27 C**) and A375 (**figure 27 D**) invasion after 24 h experiment in normoxic condition but their dissemination significantly got slower after C22 treatment. However, in accordance with migration outcomes, the most severe consequences of SMO or GLI1 inhibition were observed under hypoxia, where both cell lines invasiveness ability was almost abolished.

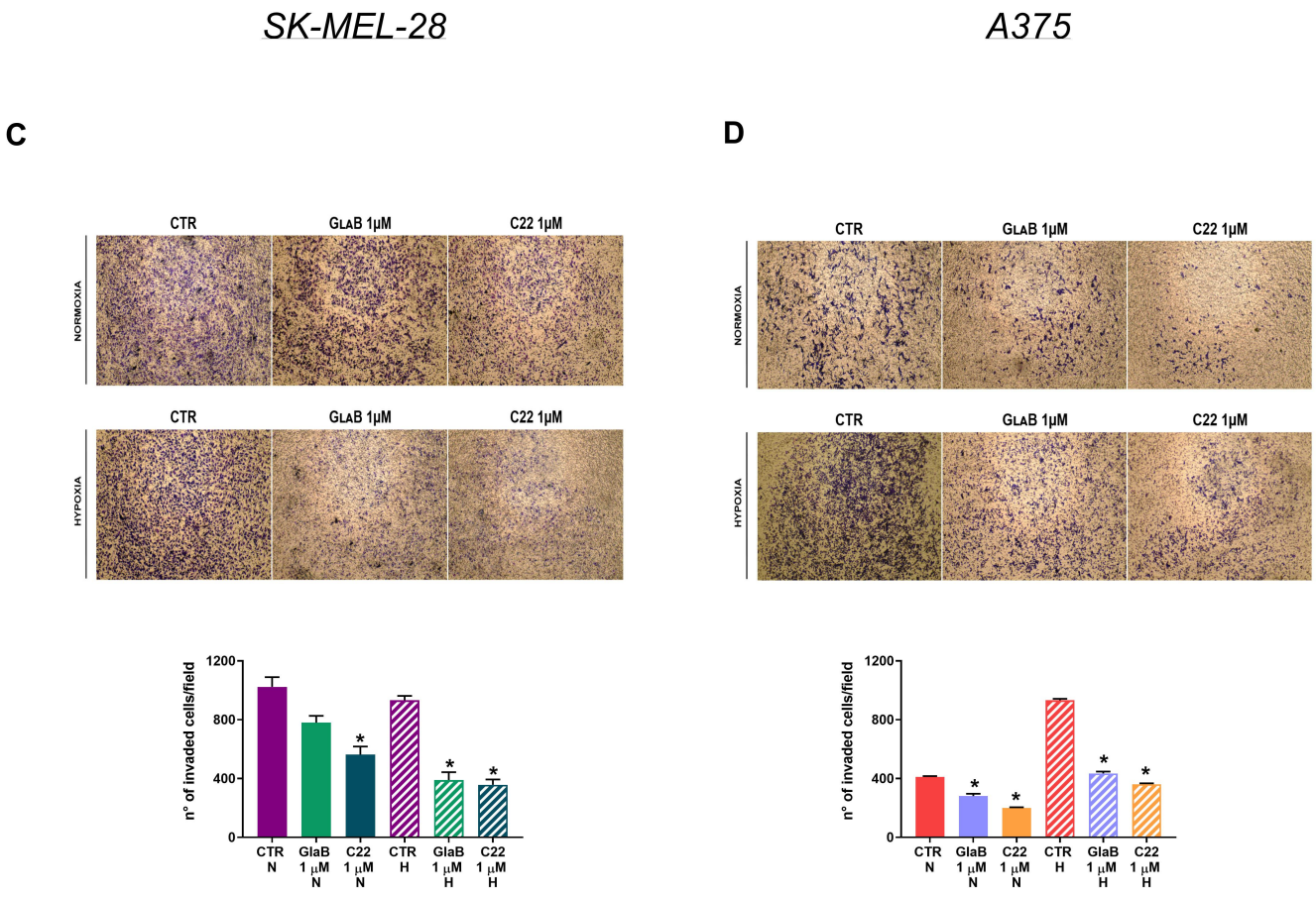

Figure 27: invasion assay with GlaB 1µM and C22 1µM treatments after 24 h under normoxic or hypoxic condition in SK-MEL-28 (**C**) and A375 (**D**). Reported pictures are representative and data are presented as the mean and ± SEM of three independent experiments. * $p \leq 0.05$ indicate statistically significant differences.

Lastly, as degradation of EMC is a fundamental step for cancer cells to disseminate, I also analyzed metalloproteinase 9 (MMP-9) activity by zymogram assay after 24 h treatment with the Hh inhibitors. **Figure 27 E** shows that GlaB treatment significantly decreased EMC degradation under hypoxia in SK-MEL-28, but the most severe effects were observed by C22 treatment, which totally blocked hypoxic MMP-9 activity. Similar effects were registered also in A375 (**figure 27 F**), where hypoxic EMC degradation was markedly affected by both SMO and GLI1 inhibitors, with no significant differences within the two treatments.

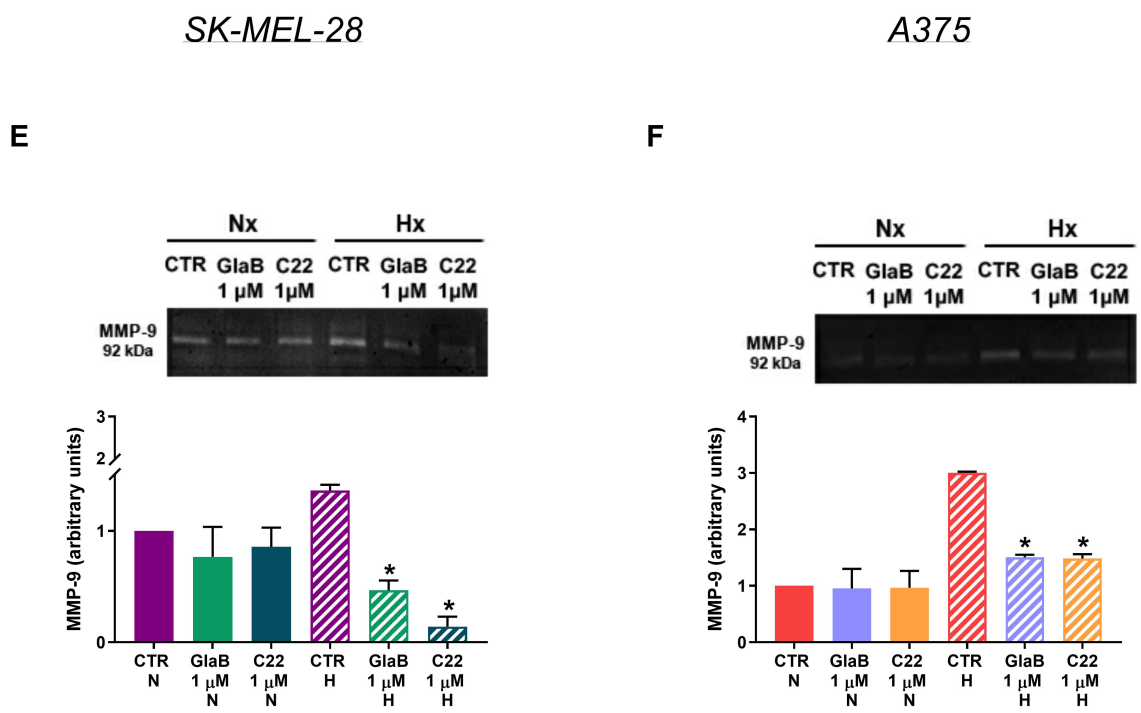

Figure 27: Zymogram blots after 24 h treatment with GlaB 1μM and C22 1μM under normoxic and hypoxic condition in SK-MEL-28 (**E**) and A375 (**F**). Reported pictures and blots are representative and data are presented as the mean and ± SEM of three independent experiments. * $p \leq 0.05$ indicate statistically significant differences.

4.6 SMO and GLI1 inhibition affected melanoma cell interaction

3-D cultures are important tools to help researchers to better understand the behavior of cancer cells in the TME. Here I tried to create monospheroids of melanoma cells with the aim to examine whether Hh inhibition resulted also in impairing tumor cell interactions. In this perspective, I cultured the two melanoma cell lines as floating spheres in ultra-low-attachment plates and monitored them until 20 days, replacing media with new treatments every two days. As **figure 28 A** shows, SK-MEL-28 CTR spheroids were almost perfectly round shape since day 1 of experiment and the sphere became increasingly compact at the end of the experiment, under both normoxia and hypoxia. Contrarily, treated spheroids never acquired a round and compact shape, with no difference within the two inhibitors used.

A similar trend was reported also by A375 (**figure 28 B**), although they struggled to remain aggregated because of their metastatic nature; however, CTR cells managed to create a round and quite compact spheroids after 20 days, while SMO and GLI1 treated cells seem to remain just cellular aggregates, without ever reaching the typical compactness of the tumor organoid. From these data emerged that inhibition of the Hh pathway at both GLI1 and SMO levels also interfered in melanoma cell-cell interaction.

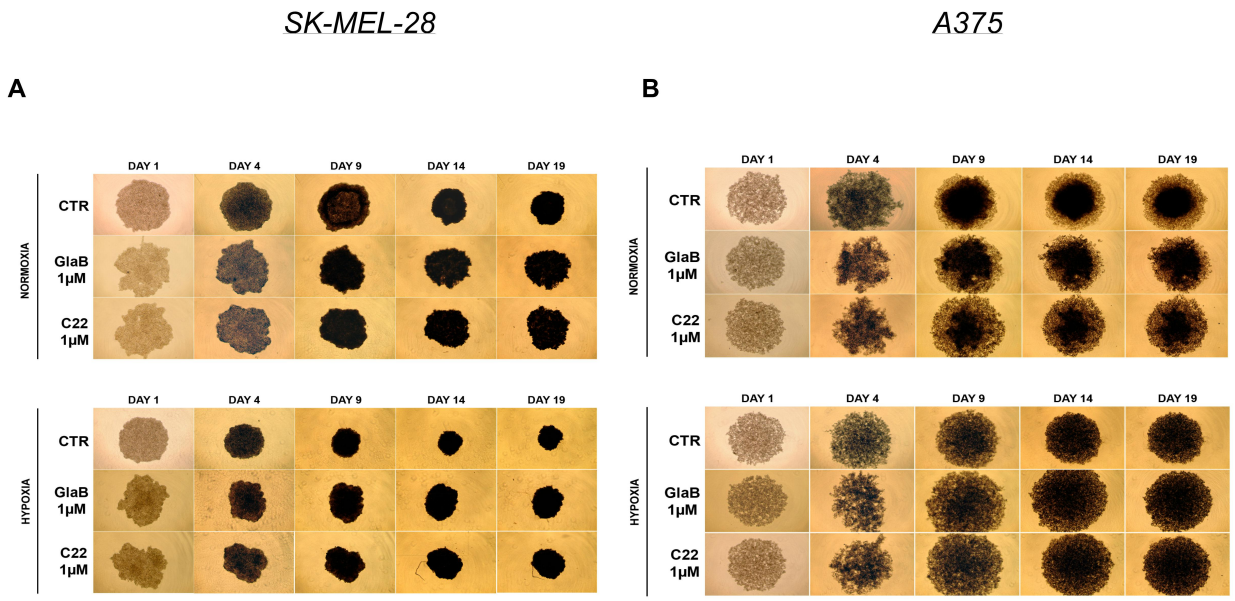

Figure 28: (**A**) SK-MEL-28 and (**B**) A375 spheroids cultured in ultra-low attachment plates and treated with GlaB 1µM and C22 1µM every two day for 20 days.

4.7 CAXII chemical inhibition impaired melanoma migration

Since both biological and chemical inhibition of the Hh pathway resulted in decreased CAXII expression, I wondered whether a direct inhibition of CAXII could impaired melanoma cell migration as well. Not only that, in the following experiments also the hypoxic isoform CAIX was introduced, to investigate if both the hypoxic CAs are involved in controlling melanoma spreading. To this end, the Department of Biotechnology, Chemistry and Pharmacy of the University of Siena kindly provided newly synthetized small molecules targeting hypoxic CAs [129], as described above: C-7 was designed to inhibit CAIX, whereas C-10 acts both on CAIX and CAXII. The pan-CAs inhibitor GV2-20 and AAZ were employed as reference compounds. As first, I tested the effects of these new compounds on SK-MEL-28 and A375 viability up to 72 h incubation, to rule out the possibility that the following migration and invasion assays might be related to cell viability variations. As shown in **figure 29 A-B**, CAs inhibitors did not significantly affect cell viability in both cell lines.

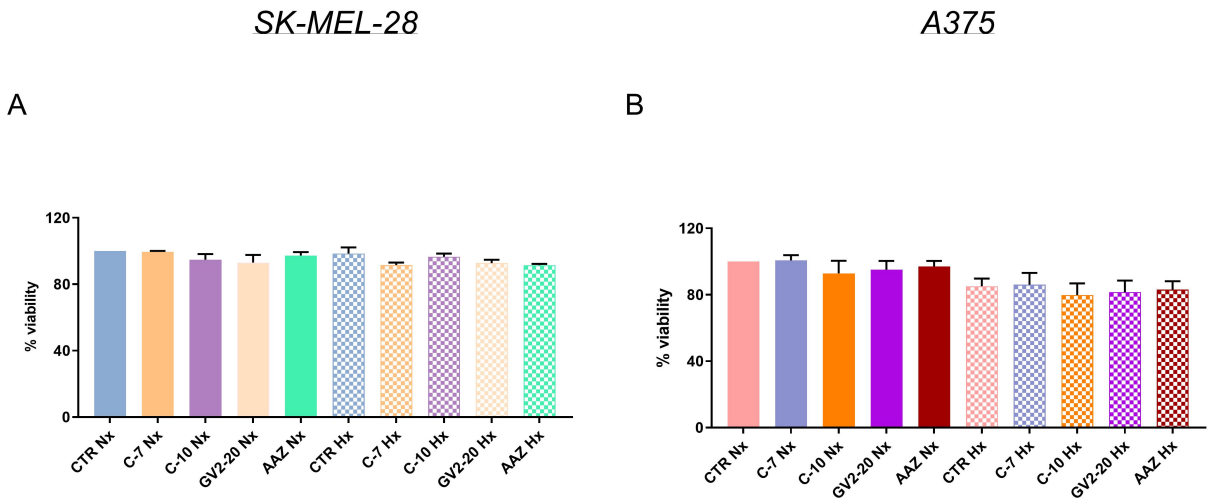

Figure 29: SK-MEL-28 (**A**) and A375 (**B**) viability assays after 72 h treatment with 10 nM of each compound and exposed to normoxia or hypoxia. Data are reported as the percentage of the ratio between the treated groups and controls. Graphs represent the means and ± SEM of the mean of three independent experiments performed in triplicates.

Therefore, I proceed to verify the effect of direct CAIX and CAXII inhibition on cell migration. From **figure 30 A** we can observe a significant reduction of SK-MEL-28 migration after 24 h treatment with C-10 under normoxia. These effects were similar also under hypoxic conditions. Instead, A375 migration was slightly impaired by C-7 treatment but the major and significantly effect was due to

C-10 inhibitor, under both normoxia and hypoxia (**figure 30 B**). These results suggested that the inhibition of CAIX alone was not sufficient to regulate melanoma cell migration. In contrast, CAXII appeared to be a key regulator in the migration of the intermediate and high aggressive melanoma cell lines. Indeed, C-10 is characterized as one of the more specific inhibitors of CAXII, when compared not only to C-7 but also to the pan-inhibitors GV2-20 and AAZ.

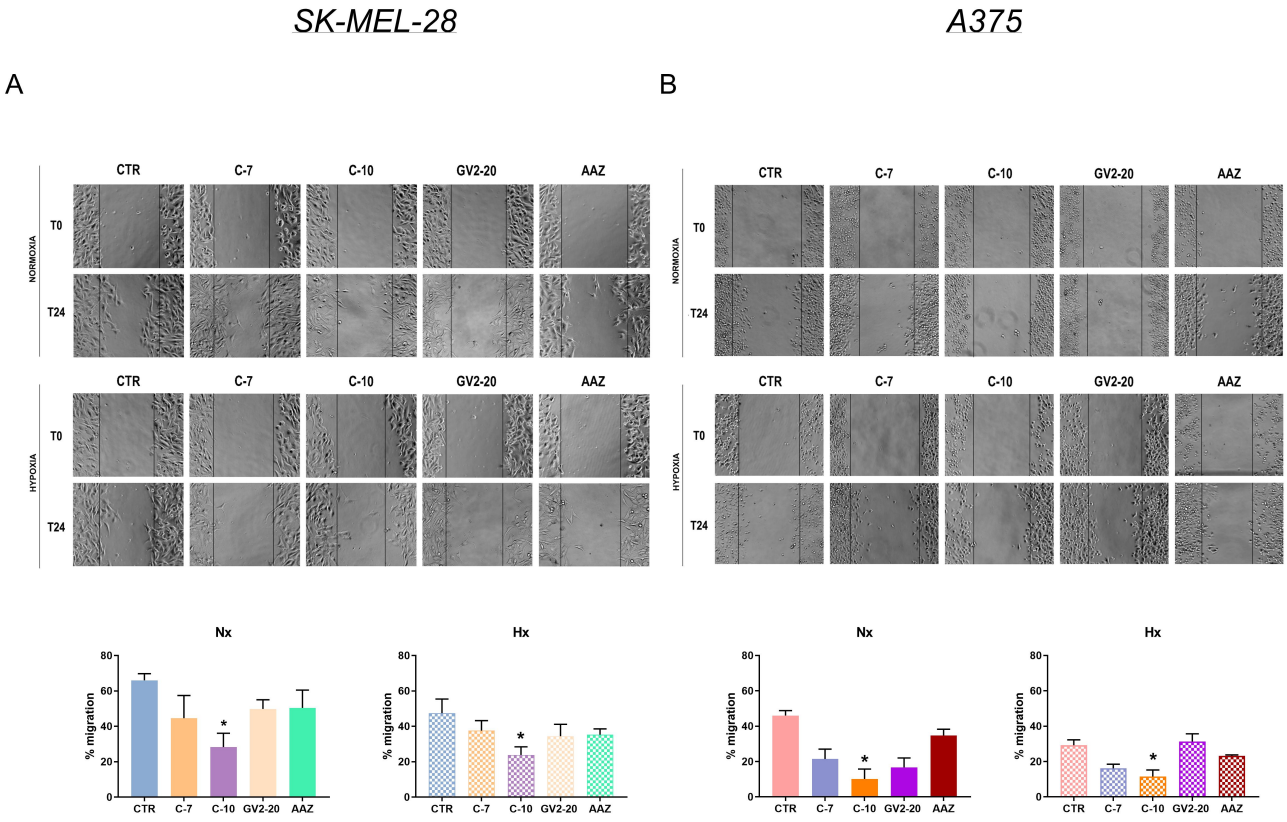

Figure 30: SK-MEL-28 (**A**) and A375 (**B**) scratch assays after 24 h treatment with 10 nM of each compound and exposed to normoxia or hypoxia. Data are represented as the percentage of migration rate between treated groups and controls. Graphs represent the means and ± SEM of the mean of three independent experiments. * $p \leq 0.05$ indicate statistically significant differences.

4.8 CAXII chemical inhibition also reduced melanoma invasion under hypoxia

At this point, analysis of the invasion ability was followed. Taking into account the above migration outcome and considering that CAIX and CAXII are isoforms not expressed or almost in normoxia and upregulated in hypoxia, the subsequent investigations related to the invasion have been taken only in the hypoxic condition. As **figure 31 A** clearly shows, C-10 treatment, unlike the pan-inhibitor AAZ, significantly reduced SK-MEL-28 invasion. A375 invasion was also significantly

impaired by both C-7 and C-10 inhibitors (**figure 31 B**) but the CAXII inhibitor resulted in the most potent effect.

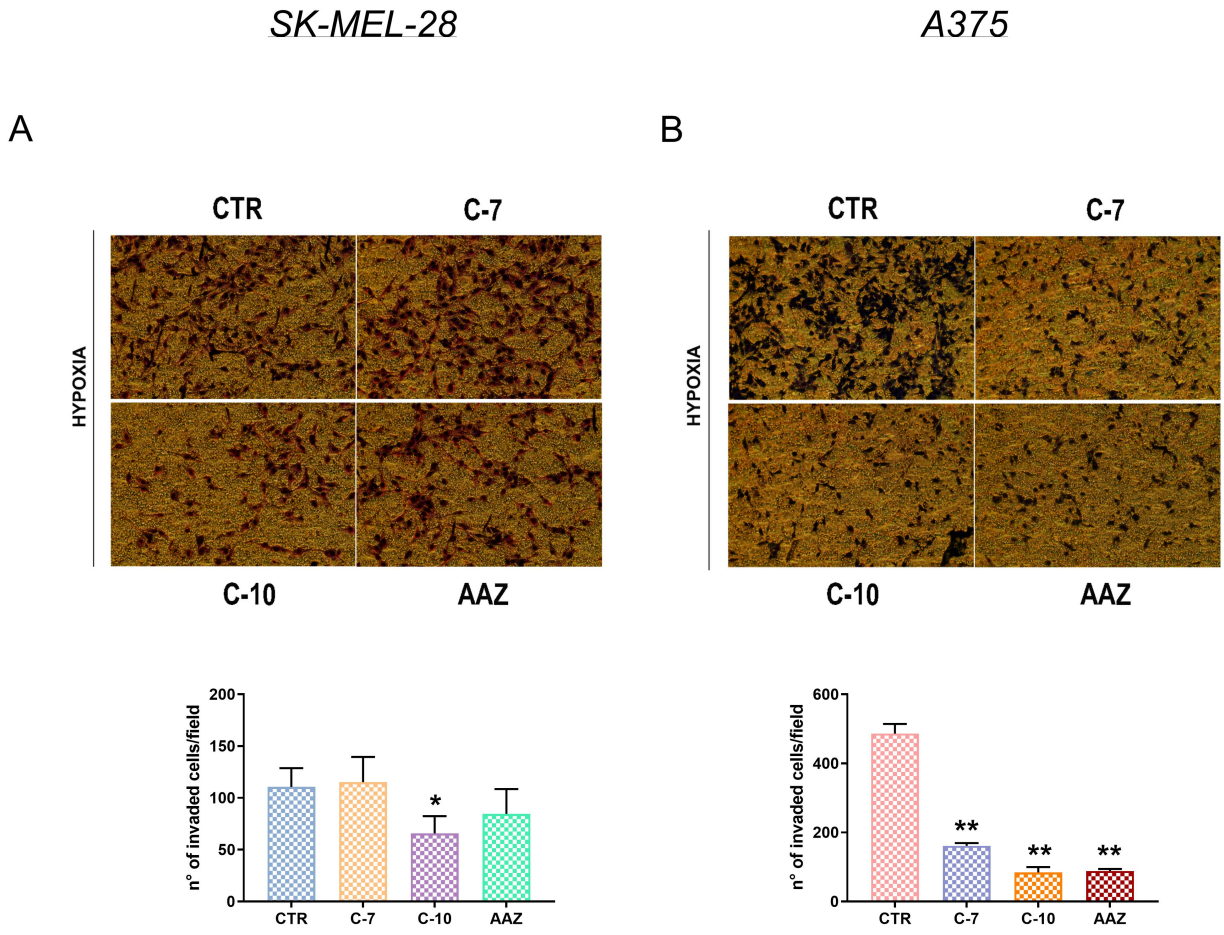

Figure 31: Modified Boyden chamber invasion assays after 24 h treatment under hypoxia in SK-MEL-28 (**A**) and A375 (**B**). Data are presented as the means and standard errors of the mean of three independent experiments performed in triplicates. Acetazolamide (AAZ) was used as control. * $p \leq 0.05$ and ** $p \leq 0.01$ indicate statistically significant differences.

Furthermore, the effects of C-7 and C-10 on the phosphorylated focal adhesion kinase (phFAK) were analyzed, as its role in the promotion of the aggressive melanoma phenotype has been previously described in several reports [134]. In line with the migration and invasion results, C-10 inhibitor significantly decreased phFAK protein levels both in SK-MEL-28 (**Figure 31 C**) and A375 (**Figure 13 D**). In addition, to support the invasion analysis, I also assessed the effect of CAIX and CAXII inhibition by the zymographic assay and C-10 treatment resulted also in a significant

decrease of MMP-9 activity, as shown in **figure 31 E-F**. However, such an inhibition was exerted also by C-7, indicating that CAIX and CAXII were similarly involved in the regulation of MMP-9.

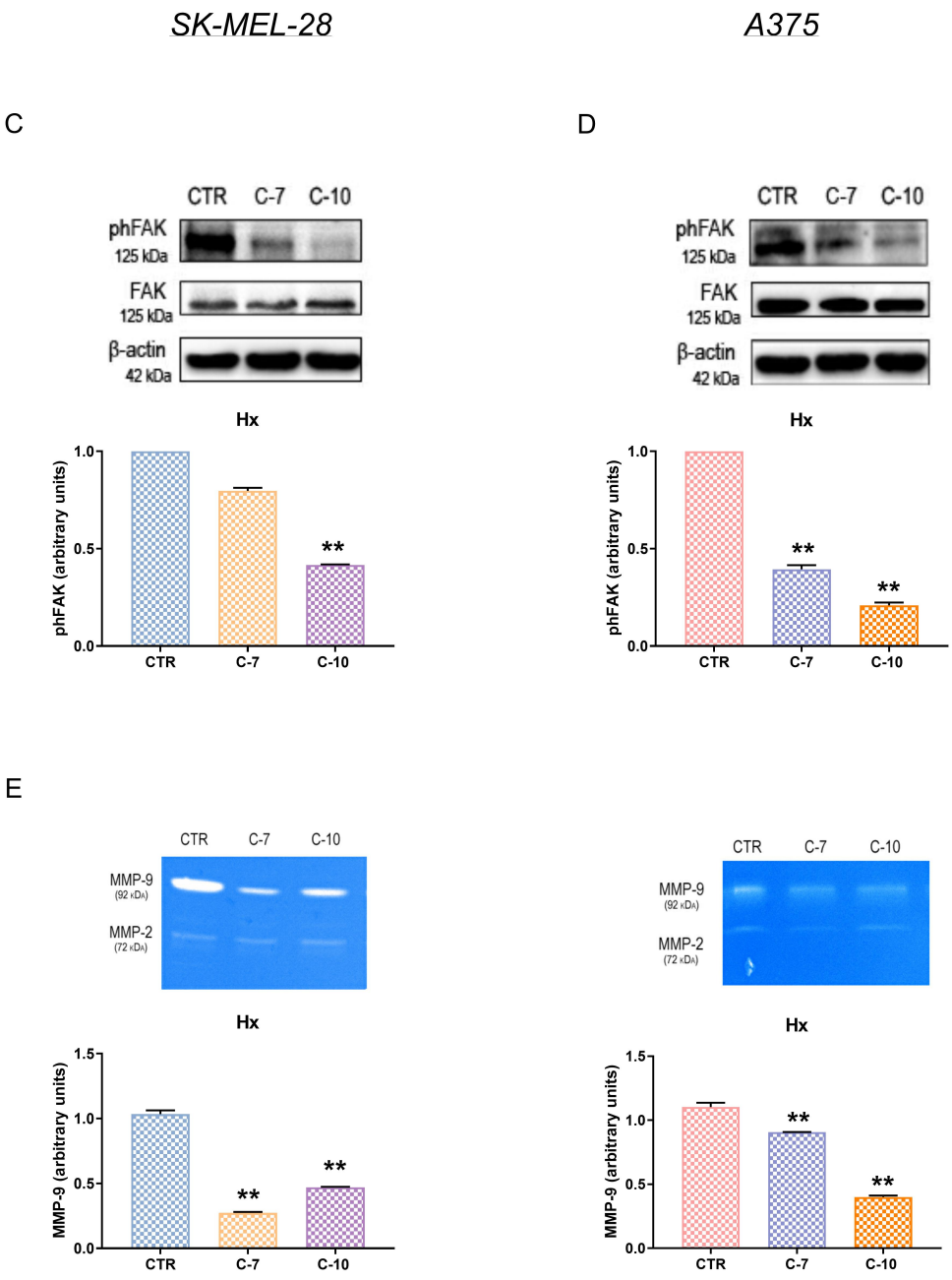

Figure 33: SK-MEL-28 (**C**) and A375 (**D**) phosphorylated focal adhesion kinase (phFAK) protein expressions after 24 h treatment with C-7 and C-10 under hypoxia. SK-MEL-28 (**E**) and A375 (**F**) matrix metalloproteinase 9 (MMP-9) enzymatic activity after 24 h treatment upon hypoxia as determined by zymography. Data are presented as the means and standard errors of the mean of three independent experiments. B-actin was used as loading control. * $p \leq 0.05$ and ** $p \leq 0.01$ indicate statistically significant differences.

5. DISCUSSION AND CONCLUSION

Tumor management is always a delicate aspect for researchers, especially in the case of highly metastatic tumors, with high mortality and drug resistance, such as melanoma. Thus, therapies for this kind of malignancy are still insufficient so that new concepts are essential.

Typical hallmarks of TME are becoming an increasingly investigated strategies and acidification is among these new targets. CAs are responsible for the acidic environment and within these, CAXII represent one of the most promising targets. Recent studied reported that CAXII expression is regulated by the Hh pathway in breast cancer [125], underlying the potential role that it plays in tumor migration. Therefore, I tried to understand if this correlation may occur also in melanoma. First, I achieved SMO and GLI1 transient silencing and analyzed two different grades of malignant melanoma migratory and invasiveness abilities. From these analyses emerged that intermediate metastatic SK-MEL-28 migration and invasion were strictly decreased by GLI1 silencing and much more by SMO knock down and these restrictions were enhanced under hypoxic condition. Even highly metastatic A375 dissemination resulted to be strictly impaired by both Hh blockades and, even in this case, the most severe consequences were shown under hypoxia. These preliminary results are in accordance with the evidence that hypoxia play crucial role in melanoma progression [90] . Non only that, but these findings are also crucial because they recognizes to the Hh pathway a role in melanoma motility, while up to now it was studied mainly for the survival for the cancer cells [135]. Then, I evaluated if SMO and GLI1 knock down resulted in CAXII modulation; surprisingly, the link between the Hh and CAXII exists also in melanoma, as inhibition of both SMO and GLI1 decreased CAXII expression. I thus hypothesized that the molecular mechanism by which the Hh pathway impairs melanoma migration and invasion would regard CAXII activity. To this aim, CAXII transient silencing was also performed and its effects on melanoma spreading examined. As expected, even in this case, CAXII knock down resulted in reducing both intermediate and highly metastatic melanoma migration, both under normoxia and much more under hypoxia. However, the hardest effects of such inhibition were observed on the infiltrative ability of melanoma. Indeed, from these data emerged that intermediate metastatic melanoma was highly susceptible to CAXII suppression, as its invasiveness ability was almost suppressed, and the effects were similar both in normoxic and hypoxic condition. On the contrary, metastatic melanoma seems to be little stimulated to invade in a normoxic environment, where however the effects of CAXII

suppression were weakly seen; whereas the hypoxic condition strongly drove highly metastatic cells to infiltrate, where the hardest effect of CAXII silencing were obtained.

Surgical resection is the typical treatment for localized melanoma and chemotherapy is the only line of defense in metastatic phase. In recent years, great progresses have been made by targeted-therapies designed on the single patient, with the aim to reduce the cytotoxic side effects provoked by a systemic chemotherapy approach [136]. In this context, several antibodies and small molecules have been designed. In this thesis the biological effects of two small GLI1 and SMO/GLI1 inhibitors (kindly provided by the Department of Chemistry and Technology of Drugs-"La Sapienza" University) were tested [126, 127]. In line with the silencing results above described, chemical Hh suppression strongly reduced both intermediate and highly metastatic migration, under both normoxic and hypoxic microenvironments and major effects were reported by the concomitant inhibition of the upstream and downstream of the Hh cascade. Similarly, invasiveness abilities were also limited with a severe suppression under hypoxia. The impaired infiltrating abilities by the Hh inhibition were also supported by the analyses of the metalloproteases activity; thus, MMP-9 resulted to be strongly reduced under hypoxic condition, especially by the simultaneous inhibition of SMO and GLI1 in the intermediate metastatic cell line. This may indicate that in highly metastatic melanoma the propensity to spread is so high that it makes no difference whether Hh suppression depends on SMO or GLI1 activity, while on the contrary, for the medially metastatic tumor, the infiltrative feature is more stimulated by SMO activity.

Moreover, established the effects of these new small Hh inhibitors in motility and invasiveness, I controlled if CAXII expression could be also impaired. Again, in accordance with the silencing results, CAXII expression resulted hardly decreased by both SMO and GLI1 inhibition and the effects were obtained under both normoxia and hypoxia. These results may open a new scenario in melanoma management, using the Hh pathway as a mean to blockade CAXII, and so melanoma metastasis.

At this point, after obtaining an indirect inhibition of CAXII through the Hh, I tried to evaluate a direct strategy for CAXII suppression; thus, the Department of Biotechnology, Chemistry and Pharmacy-University of Siena kindly provided newly designed small inhibitors targeting CAIX or CAXII/CAIX simultaneously and again I evaluated them in term of migration and invasion. What I obtained was that simultaneously inhibition of CAXII and CAIX was able to reduce cell migration while only CAIX inhibition of by C-7 was not sufficient. This result highlights the crucial role that

CAXII, and not CAIX, play in melanoma migration. In addition, here it is observed that CAXII inhibition was particularly effective also in reducing the invasion of both intermediate and highly metastatic melanoma, under the hypoxic condition that mimics the TME. It should be pointed out that this thesis is an assessment of a possible new therapeutic strategy, reason why the experiments relating to the invasive capacity of the tumor were performed only under hypoxia, the microenvironment where CAXII is overexpressed. Eventually, infiltrating analysis was supported by the evidence that C-10 reduced the phosphorylation of FAK, as well as the activity of MMP-9. Since both FAK and MMP-9 have been previously related to the invasive properties of melanoma cells, these results further support the anti-invasive properties of CAXII inhibition.

To conclude, with this dissertation it has been preliminarily reported that in melanoma there is an interaction between SMO, GLI1 and CAXII; CAXII, and not CAIX, is responsible for the migration and invasion of metastatic melanoma; finally, it has been brought to light two different mechanisms with which to highlight CAXII as therapeutic target: a direct inhibition approach and an indirect inhibition, through the inhibition of the Hh cascade.

6. ABBREVIATIONS

ATP	Adenosine triphosphate
BCC	Basal cell carcinoma
BRAFi	BRAF inhibitor
CAIX	Carbonic anhydrase IX
CAXII	Carbonic anhydrase XII
CDK4	Cyclin dependent kinase
CDKN2A	Cyclin dependent kinase inhibitor 2A
cDNA	complementary DNA
CK1	Casein kinase 1
CO_2	Carbon dioxide
CTLA-4	Cytotoxic T-Lymphocyte Antigen 4
DHh	Desert Hedgehog
DISP	Dispatched
DMSO	Dimethyl sulfoxide
ECM	Extracellular matrix
EMT	Epithelial-to-mesenchymal transition
EPO	Erythropoietin
ER	Endoplasmic reticulum
FDA	Food and Drug Administration
FIH	Factor inhibiting HIF
GLAB	Glabrescione B
GLI	Glioma-associated oncogene protein
GLIA	Glioma-associated oncogene protein activator
GPCR	G-protein coupled receptor
GSK3β	Glycogen synthase kinase 3β
Hh	Hedgehog
HIF	Hypoxia-inducible factor
HRE	Hypoxia Responsive Elements
IFN- γ	Iinterferon γ

IFT	Intraflagellar transport system
IGF	Insulin-like growth factor
IHC	Immunohistochemistry
IHh	Indian Hedgehog
JNK	Jun N-terminal kinase
KIF7	Kinesin family member
MC1R	Melacortin 1 receptor
MEKi	MEK inhibitor
MIFT	Melanocyte Inducing Transcription Factor
MMP	Matrix metalloproteinase
O_2	Oxygen
OXPHOS	Oxidative phosphorylation
PATCH	Patched
PBS	Phosphate buffered saline
PHD	Prolyl hydroxylases
PI	Primary cilium
PKA	Protein kinase A
pVHL	von Hippel-Lindau protein
SCC	Squamos cell carcinoma
SHh	Sonic Hedgehog
SMO	Smoothened
SOX10	SRY-Box Transcription Factor 10
SuFu	Suppressor of Fu
TME	Tumor microenvironment
UVR	Ultraviolet radiation
VEGF	vascular endothelial cell growth factor
WHO	World Health Organization
α MSH	alpha melanocyte stimulating hormone
αSMA	alpha smooth muscle actin

7. REFERENCES

1. Gordon, R. *Skin cancer: an overview of epidemiology and risk factors*. in *Seminars in oncology nursing*. 2013: Elsevier.
2. Rebecca, V.W., V.K. Sondak, and K.S. Smalley, *A brief history of melanoma: from mummies to mutations.* Melanoma research, 2012. **22**(2): p. 114.
3. Sung, H., et al., *Global cancer statistics 2020: GLOBOCAN estimates of incidence and mortality worldwide for 36 cancers in 185 countries.* CA: a cancer journal for clinicians, 2021. **71**(3): p. 209-249.
4. Williams, P.F., et al., *Melanocortin 1 receptor and risk of cutaneous melanoma: A meta-analysis and estimates of population burden.* International Journal of Cancer, 2011. **129**(7): p. 1730-1740.
5. Seiberg, M., *Keratinocyte–melanocyte interactions during melanosome transfer.* Pigment Cell Research, 2001. **14**(4): p. 236-242.
6. Hida, T., et al., *Elucidation of melanogenesis cascade for identifying pathophysiology and therapeutic approach of pigmentary disorders and melanoma.* International journal of molecular sciences, 2020. **21**(17): p. 6129.
7. Bastian, B.C., *The molecular pathology of melanoma: an integrated taxonomy of melanocytic neoplasia.* Annual Review of Pathology: Mechanisms of Disease, 2014. **9**: p. 239-271.
8. Hodis, E., et al., *A landscape of driver mutations in melanoma.* Cell, 2012. **150**(2): p. 251-263.
9. Bevona, C., et al., *Cutaneous melanomas associated with nevi.* Archives of dermatology, 2003. **139**(12): p. 1620-1624.
10. Dessinioti, C., et al., *Melanocortin 1 receptor variants: functional role and pigmentary associations.* Photochemistry and photobiology, 2011. **87**(5): p. 978-987.
11. Rossi, M., et al., *Familial melanoma: diagnostic and management implications.* Dermatology practical & conceptual, 2019. **9**(1): p. 10.
12. Goldstein, A.M. and M.A. Tucker, *Genetic epidemiology of cutaneous melanoma: a global perspective.* Archives of dermatology, 2001. **137**(11): p. 1493-1496.
13. Zaidi, M.R., et al., *Interferon-γ links ultraviolet radiation to melanomagenesis in mice.* Nature, 2011. **469**(7331): p. 548-553.
14. Dérijard, B., et al., *JNK1: a protein kinase stimulated by UV light and Ha-Ras that binds and phosphorylates the c-Jun activation domain.* Cell, 1994. **76**(6): p. 1025-1037.
15. Flaherty, K.T., F.S. Hodi, and D.E. Fisher, *From genes to drugs: targeted strategies for melanoma.* Nature Reviews Cancer, 2012. **12**(5): p. 349-361.
16. Chin, L., L.A. Garraway, and D.E. Fisher, *Malignant melanoma: genetics and therapeutics in the genomic era.* Genes & development, 2006. **20**(16): p. 2149-2182.
17. Teixido, C., et al., *Molecular markers and targets in melanoma.* Cells, 2021. **10**(9): p. 2320.
18. Ferrara, G. and G. Argenziano, *The WHO 2018 Classification of Cutaneous Melanocytic Neoplasms: Suggestions From Routine Practice.* Frontiers in oncology, 2021. **11**.
19. Castillo, P., et al., *Implementation of an NGS panel for clinical practice in paraffin-embedded tissue samples from locally advanced and metastatic melanoma patients.* Explor. Target Antitumor Ther, 2020. **1**: p. 101-108.

20. Nazarian, R., et al., *Melanomas acquire resistance to B-RAF (V600E) inhibition by RTK or N-RAS upregulation.* Nature, 2010. **468**(7326): p. 973-977.
21. Rosenberg, S.A. and N.P. Restifo, *Adoptive cell transfer as personalized immunotherapy for human cancer.* Science, 2015. **348**(6230): p. 62-68.
22. Christodoulou, E., et al., *Analysis of CRISPR-Cas9 screens identifies genetic dependencies in melanoma.* Pigment cell & melanoma research, 2021. **34**(1): p. 122.
23. Nüsslein-Volhard, C. and E. Wieschaus, *Mutations affecting segment number and polarity in Drosophila.* Nature, 1980. **287**(5785): p. 795-801.
24. Jiang, J. and C.-c. Hui, *Hedgehog signaling in development and cancer.* Developmental cell, 2008. **15**(6): p. 801-812.
25. Riobo, N.A. and D.R. Manning, *Pathways of signal transduction employed by vertebrate Hedgehogs.* Biochemical journal, 2007. **403**(3): p. 369-379.
26. Ahn, S. and A.L. Joyner, *In vivo analysis of quiescent adult neural stem cells responding to Sonic hedgehog.* Nature, 2005. **437**(7060): p. 894-897.
27. Ihrie, R.A., et al., *Persistent sonic hedgehog signaling in adult brain determines neural stem cell positional identity.* Neuron, 2011. **71**(2): p. 250-262.
28. Brownell, I., et al., *Nerve-derived sonic hedgehog defines a niche for hair follicle stem cells capable of becoming epidermal stem cells.* Cell stem cell, 2011. **8**(5): p. 552-565.
29. Peng, Y.-C., et al., *Sonic hedgehog signals to multiple prostate stromal stem cells that replenish distinct stromal subtypes during regeneration.* Proceedings of the national academy of sciences, 2013. **110**(51): p. 20611-20616.
30. Shin, K., et al., *Hedgehog/Wnt feedback supports regenerative proliferation of epithelial stem cells in bladder.* Nature, 2011. **472**(7341): p. 110-114.
31. Carballo, G.B., J.R. Honorato, and G.P.F. de Lopes, *A highlight on Sonic hedgehog pathway.* Cell Communication and Signaling, 2018. **16**(1): p. 1-15.
32. Bitgood, M.J., L. Shen, and A.P. McMahon, *Sertoli cell signaling by Desert hedgehog regulates the male germline.* Current biology, 1996. **6**(3): p. 298-304.
33. Wijgerde, M., et al., *Hedgehog signaling in mouse ovary: Indian hedgehog and desert hedgehog from granulosa cells induce target gene expression in developing theca cells.* Endocrinology, 2005. **146**(8): p. 3558-3566.
34. Chamoun, Z., et al., *Skinny hedgehog, an acyltransferase required for palmitoylation and activity of the hedgehog signal.* Science, 2001. **293**(5537): p. 2080-2084.
35. Gallet, A., et al., *Cholesterol modification of hedgehog is required for trafficking and movement, revealing an asymmetric cellular response to hedgehog.* Developmental cell, 2003. **4**(2): p. 191-204.
36. Choudhry, Z., et al., *Sonic hedgehog signalling pathway: a complex network.* Annals of neurosciences, 2014. **21**(1): p. 28.
37. Briscoe, J. and P.P. Thérond, *The mechanisms of Hedgehog signalling and its roles in development and disease.* Nature reviews Molecular cell biology, 2013. **14**(7): p. 416-429.
38. Petrova, R. and A.L. Joyner, *Roles for Hedgehog signaling in adult organ homeostasis and repair.* Development, 2014. **141**(18): p. 3445-3457.
39. Gigante, E.D. and T. Caspary, *Signaling in the primary cilium through the lens of the Hedgehog pathway.* Wiley Interdisciplinary Reviews: Developmental Biology, 2020. **9**(6): p. e377.
40. Chai, J.Y., et al., *Defining the Role of GLI/Hedgehog Signaling in Chemoresistance: Implications in Therapeutic Approaches.* Cancers, 2021. **13**(19): p. 4746.

41. Yang, L., et al., *Activation of the hedgehog-signaling pathway in human cancer and the clinical implications.* Oncogene, 2010. **29**(4): p. 469-481.
42. Skoda, A.M., et al., *The role of the Hedgehog signaling pathway in cancer: A comprehensive review.* Bosnian journal of basic medical sciences, 2018. **18**(1): p. 8.
43. Brennan, D., et al., *Noncanonical hedgehog signaling.* Vitamins & Hormones, 2012. **88**: p. 55-72.
44. Teperino, R., et al. *Canonical and non-canonical Hedgehog signalling and the control of metabolism*. in *Seminars in cell & developmental biology*. 2014: Elsevier.
45. Jeng, K.-S., C.-F. Chang, and S.-S. Lin, *Sonic hedgehog signaling in organogenesis, tumors, and tumor microenvironments.* International journal of molecular sciences, 2020. **21**(3): p. 758.
46. Araújo, S.J., *The hedgehog signalling pathway in cell migration and guidance: what we have learned from Drosophila melanogaster.* Cancers, 2015. **7**(4): p. 2012-2022.
47. Katoh, Y. and M. Katoh, *Hedgehog target genes: mechanisms of carcinogenesis induced by aberrant hedgehog signaling activation.* Current molecular medicine, 2009. **9**(7): p. 873-886.
48. Chen, J.-S., et al., *Sonic hedgehog signaling pathway induces cell migration and invasion through focal adhesion kinase/AKT signaling-mediated activation of matrix metalloproteinase (MMP)-2 and MMP-9 in liver cancer.* Carcinogenesis, 2013. **34**(1): p. 10-19.
49. Polizio, A.H., et al., *Heterotrimeric Gi proteins link Hedgehog signaling to activation of Rho small GTPases to promote fibroblast migration.* Journal of Biological Chemistry, 2011. **286**(22): p. 19589-19596.
50. Kinzler, K.W., et al., *Identification of an amplified, highly expressed gene in a human glioma.* Science, 1987. **236**(4797): p. 70-73.
51. Amakye, D., Z. Jagani, and M. Dorsch, *Unraveling the therapeutic potential of the Hedgehog pathway in cancer.* Nature medicine, 2013. **19**(11): p. 1410-1422.
52. Clement, V., et al., *HEDGEHOG-GLI1 signaling regulates human glioma growth, cancer stem cell self-renewal, and tumorigenicity.* Current biology, 2007. **17**(2): p. 165-172.
53. Yauch, R.L., et al., *A paracrine requirement for hedgehog signalling in cancer.* Nature, 2008. **455**(7211): p. 406-410.
54. Peng, Z.-P., et al., *The Effects of Hedgehog Signaling Pathway on the Proliferation and Apoptosis of Melanoma Cells.* Journal of Oncology, 2022. **2022**.
55. Duan, F., et al., *Effects of inhibition of hedgehog signaling on cell growth and migration of uveal melanoma cells.* Cancer biology & therapy, 2014. **15**(5): p. 544-559.
56. Chen, J., et al., *Circ-GLI1 promotes metastasis in melanoma through interacting with p70S6K2 to activate Hedgehog/GLI1 and Wnt/β-catenin pathways and upregulate Cyr61.* Cell death & disease, 2020. **11**(7): p. 1-16.
57. Semenza, G.L., *Oxygen homeostasis.* Wiley Interdisciplinary Reviews: Systems Biology and Medicine, 2010. **2**(3): p. 336-361.
58. Semenza, G.L., *Hypoxia-inducible factors in physiology and medicine.* Cell, 2012. **148**(3): p. 399-408.
59. Taylor, C.T., *Mitochondria and cellular oxygen sensing in the HIF pathway.* Biochemical journal, 2008. **409**(1): p. 19-26.
60. Cummins, E.P., et al., *The role of HIF in immunity and inflammation.* Molecular aspects of medicine, 2016. **47**: p. 24-34.

61. Wang, G.L., et al., *Hypoxia-inducible factor 1 is a basic-helix-loop-helix-PAS heterodimer regulated by cellular O2 tension.* Proceedings of the national academy of sciences, 1995. **92**(12): p. 5510-5514.
62. Kaelin Jr, W.G. and P.J. Ratcliffe, *Oxygen sensing by metazoans: the central role of the HIF hydroxylase pathway.* Molecular cell, 2008. **30**(4): p. 393-402.
63. Jiang, B.-H., et al., *Dimerization, DNA binding, and transactivation properties of hypoxia-inducible factor 1.* Journal of Biological Chemistry, 1996. **271**(30): p. 17771-17778.
64. Hu, C.-J., et al., *Differential roles of hypoxia-inducible factor 1α (HIF-1α) and HIF-2α in hypoxic gene regulation.* Molecular and cellular biology, 2003. **23**(24): p. 9361-9374.
65. Maxwell, P.H., et al., *The tumour suppressor protein VHL targets hypoxia-inducible factors for oxygen-dependent proteolysis.* Nature, 1999. **399**(6733): p. 271-275.
66. Semenza, G.L., *Involvement of hypoxia-inducible factor 1 in human cancer.* Internal medicine, 2002. **41**(2): p. 79-83.
67. Albadari, N., S. Deng, and W. Li, *The transcriptional factors HIF-1 and HIF-2 and their novel inhibitors in cancer therapy.* Expert opinion on drug discovery, 2019. **14**(7): p. 667-682.
68. Semenza, G.L., et al., *Hypoxia-inducible nuclear factors bind to an enhancer element located 3'to the human erythropoietin gene.* Proceedings of the national academy of sciences, 1991. **88**(13): p. 5680-5684.
69. Neufeld, G., et al., *Vascular endothelial growth factor (VEGF) and its receptors.* The FASEB journal, 1999. **13**(1): p. 9-22.
70. Ke, Q. and M. Costa, *Hypoxia-inducible factor-1 (HIF-1).* Molecular pharmacology, 2006. **70**(5): p. 1469-1480.
71. Michiels, C., *Physiological and pathological responses to hypoxia.* The American journal of pathology, 2004. **164**(6): p. 1875-1882.
72. West, J.B., *The physiologic basis of high-altitude diseases.* Annals of internal medicine, 2004. **141**(10): p. 789-800.
73. West, J.B., et al., *Pulmonary gas exchange on the summit of Mount Everest.* Journal of applied physiology, 1983. **55**(3): p. 678-687.
74. Pedersen, B.K. and A. Steensberg, *Exercise and hypoxia: effects on leukocytes and interleukin-6—shared mechanisms?* Medicine & Science in Sports & Exercise, 2002. **34**(12): p. 2004-2012.
75. Braun, R.D., et al., *Comparison of tumor and normal tissue oxygen tension measurements using OxyLite or microelectrodes in rodents.* American Journal of Physiology-Heart and Circulatory Physiology, 2001. **280**(6): p. H2533-H2544.
76. Spencer, J.A., et al., *Direct measurement of local oxygen concentration in the bone marrow of live animals.* Nature, 2014. **508**(7495): p. 269-273.
77. Harrison, J.S., et al., *Oxygen saturation in the bone marrow of healthy volunteers.* Blood, The Journal of the American Society of Hematology, 2002. **99**(1): p. 394-394.
78. Huang, J.H., et al., *Requirements for T lymphocyte migration in explanted lymph nodes.* The Journal of Immunology, 2007. **178**(12): p. 7747-7755.
79. Taylor, C.T. and S.P. Colgan, *Regulation of immunity and inflammation by hypoxia in immunological niches.* Nature Reviews Immunology, 2017. **17**(12): p. 774-785.
80. Semenza, G.L., *HIF-1: upstream and downstream of cancer metabolism.* Current opinion in genetics & development, 2010. **20**(1): p. 51-56.
81. Schoch, H.J., S. Fischer, and H.H. Marti, *Hypoxia-induced vascular endothelial growth factor expression causes vascular leakage in the brain.* Brain, 2002. **125**(11): p. 2549-2557.

82. Oechmichen, M. and C. Meissner, *Cerebral hypoxia and ischemia: the forensic point of view: a review.* Journal of forensic sciences, 2006. **51**(4): p. 880-887.
83. Ye, J., *Emerging role of adipose tissue hypoxia in obesity and insulin resistance.* International journal of obesity, 2009. **33**(1): p. 54-66.
84. Giordano, F.J., *Oxygen, oxidative stress, hypoxia, and heart failure.* The Journal of clinical investigation, 2005. **115**(3): p. 500-508.
85. Evans, S.M., et al., *Oxygen levels in normal and previously irradiated human skin as assessed by EF5 binding.* Journal of Investigative Dermatology, 2006. **126**(12): p. 2596-2606.
86. Mouriaux, F., et al., *Increased HIF-1α expression correlates with cell proliferation and vascular markers CD31 and VEGF-A in uveal melanoma.* Investigative ophthalmology & visual science, 2014. **55**(3): p. 1277-1283.
87. Lartigau, E., et al., *Intratumoral oxygen tension in metastatic melanoma.* Melanoma research, 1997. **7**(5): p. 400-406.
88. Maadi, H., et al., *Multimodal tumor suppression by miR-302 cluster in melanoma and colon cancer.* The international journal of biochemistry & cell biology, 2016. **81**: p. 121-132.
89. Murphy, M., et al., *Hypoxia-induced response of cell cycle and apoptosis regulators in melanoma.* International journal of dermatology, 2012. **51**(10): p. 1263-1267.
90. Dratkiewicz, E., et al., *Hypoxia and Extracellular Acidification as Drivers of Melanoma Progression and Drug Resistance.* Cells, 2021. **10**(4): p. 862.
91. De Palma, M., D. Biziato, and T.V. Petrova, *Microenvironmental regulation of tumour angiogenesis.* Nature Reviews Cancer, 2017. **17**(8): p. 457-474.
92. Comito, G., et al., *Stromal fibroblasts synergize with hypoxic oxidative stress to enhance melanoma aggressiveness.* Cancer letters, 2012. **324**(1): p. 31-41.
93. Levy, C., M. Khaled, and D.E. Fisher, *MITF: master regulator of melanocyte development and melanoma oncogene.* Trends in molecular medicine, 2006. **12**(9): p. 406-414.
94. Li, H., et al., *Nodal induced by hypoxia exposure contributes to dacarbazine resistance and the maintenance of stemness in melanoma cancer stem-like cells.* Oncology reports, 2018. **39**(6): p. 2855-2864.
95. Asnaghi, L., et al., *Hypoxia promotes uveal melanoma invasion through enhanced Notch and MAPK activation.* PloS one, 2014. **9**(8): p. e105372.
96. Liu, S., et al., *Snail1 mediates hypoxia-induced melanoma progression.* The American journal of pathology, 2011. **179**(6): p. 3020-3031.
97. Cowden Dahl, K.D., et al., *Hypoxia-inducible factor regulates αvβ3 integrin cell surface expression.* Molecular biology of the cell, 2005. **16**(4): p. 1901-1912.
98. Rezvani, H.R., et al., *HIF-1α in epidermis: oxygen sensing, cutaneous angiogenesis, cancer, and non-cancer disorders.* Journal of Investigative Dermatology, 2011. **131**(9): p. 1793-1805.
99. Chung, H., et al., *Keratinocyte-derived laminin-332 promotes adhesion and migration in melanocytes and melanoma.* Journal of Biological Chemistry, 2011. **286**(15): p. 13438-13447.
100. Eble, J.A. and S. Niland, *The extracellular matrix in tumor progression and metastasis.* Clinical & experimental metastasis, 2019. **36**(3): p. 171-198.
101. Lindskog, S., *Structure and mechanism of carbonic anhydrase.* Pharmacology & therapeutics, 1997. **74**(1): p. 1-20.
102. Supuran, C.T., *Carbonic anhydrases: novel therapeutic applications for inhibitors and activators.* Nature reviews Drug discovery, 2008. **7**(2): p. 168-181.

103. Lomelino, C.L., C.T. Supuran, and R. McKenna, *Non-classical inhibition of carbonic anhydrase.* International journal of molecular sciences, 2016. **17**(7): p. 1150.
104. Supuran, C.T., *Carbonic anhydrases-an overview.* Current pharmaceutical design, 2008. **14**(7): p. 603-614.
105. Waheed, A. and W.S. Sly, *Carbonic anhydrase XII functions in health and disease.* Gene, 2017. **623**: p. 33-40.
106. Pastorekova, S., et al., *Carbonic anhydrase IX, MN/CA IX: analysis of stomach complementary DNA sequence and expression in human and rat alimentary tracts.* Gastroenterology, 1997. **112**(2): p. 398-408.
107. Parkkila, S., et al., *Expression of the membrane-associated carbonic anhydrase isozyme XII in the human kidney and renal tumors.* Journal of Histochemistry & Cytochemistry, 2000. **48**(12): p. 1601-1608.
108. Ivanov, S., et al., *Expression of hypoxia-inducible cell-surface transmembrane carbonic anhydrases in human cancer.* The American journal of pathology, 2001. **158**(3): p. 905-919.
109. Barnett, D.H., et al., *Estrogen receptor regulation of carbonic anhydrase XII through a distal enhancer in breast cancer.* Cancer research, 2008. **68**(9): p. 3505-3515.
110. Williams, K.J. and R.G. Gieling, *Preclinical evaluation of ureidosulfamate carbonic anhydrase IX/XII inhibitors in the treatment of cancers.* International journal of molecular sciences, 2019. **20**(23): p. 6080.
111. Singh, S., et al., *Cancer drug development of carbonic anhydrase inhibitors beyond the active site.* Molecules, 2018. **23**(5): p. 1045.
112. Pastorekova, S. and C.T. Supuran, *Carbonic anhydrase IX: from biology to therapy*, in *Hypoxia and cancer*. 2014, Springer. p. 121-153.
113. Radvak, P., et al., *Suppression of carbonic anhydrase IX leads to aberrant focal adhesion and decreased invasion of tumor cells.* Oncology reports, 2013. **29**(3): p. 1147-1153.
114. Alblazi, K.M.O. and C.H. Siar, *Cellular protrusions-lamellipodia, filopodia, invadopodia and podosomes-and their roles in progression of orofacial tumours: current understanding.* Asian Pacific Journal of Cancer Prevention, 2015. **16**(6): p. 2187-2191.
115. Horie, K., et al., *Exosomes expressing carbonic anhydrase 9 promote angiogenesis.* Biochemical and biophysical research communications, 2017. **492**(3): p. 356-361.
116. Choschzick, M., et al., *Overexpression of carbonic anhydrase IX (CAIX) is an independent unfavorable prognostic marker in endometrioid ovarian cancer.* Virchows Archiv, 2011. **459**(2): p. 193-200.
117. Pinheiro, C., et al., *GLUT1 and CAIX expression profiles in breast cancer correlate with adverse prognostic factors and MCT1 overexpression.* 2011.
118. Klatte, T., et al., *Carbonic anhydrase IX in bladder cancer: a diagnostic, prognostic, and therapeutic molecular marker.* Cancer: Interdisciplinary International Journal of the American Cancer Society, 2009. **115**(7): p. 1448-1458.
119. Ilie, M., et al., *High levels of carbonic anhydrase IX in tumour tissue and plasma are biomarkers of poor prognostic in patients with non-small cell lung cancer.* British journal of cancer, 2010. **102**(11): p. 1627-1635.
120. Türeci, Ö., et al., *Human carbonic anhydrase XII: cDNA cloning, expression, and chromosomal localization of a carbonic anhydrase gene that is overexpressed in some renal cell cancers.* Proceedings of the national academy of sciences, 1998. **95**(13): p. 7608-7613.
121. Ivanov, S.V., et al., *Down-regulation of transmembrane carbonic anhydrases in renal cell carcinoma cell lines by wild-type von Hippel-Lindau transgenes.* Proceedings of the national academy of sciences, 1998. **95**(21): p. 12596-12601.

122. Wykoff, C.C., et al., *Expression of the hypoxia-inducible and tumor-associated carbonic anhydrases in ductal carcinoma in situ of the breast.* The American journal of pathology, 2001. **158**(3): p. 1011-1019.
123. Haapasalo, J., et al., *Identification of an alternatively spliced isoform of carbonic anhydrase XII in diffusely infiltrating astrocytic gliomas.* Neuro-oncology, 2008. **10**(2): p. 131-138.
124. Kivelä, A., et al., *Expression of a novel transmembrane carbonic anhydrase isozyme XII in normal human gut and colorectal tumors.* The American journal of pathology, 2000. **156**(2): p. 577-584.
125. Guerrini, G., et al., *Inhibition of smoothened in breast cancer cells reduces CAXII expression and cell migration.* Journal of cellular physiology, 2018. **233**(12): p. 9799-9811.
126. Infante, P., et al., *Gli1/DNA interaction is a druggable target for Hedgehog-dependent tumors.* The EMBO journal, 2015. **34**(2): p. 200-217.
127. Lospinoso Severini, L., et al., *A smo/gli multitarget hedgehog pathway inhibitor impairs tumor growth.* Cancers, 2019. **11**(10): p. 1518.
128. Mori, M., et al., *Hit recycling: discovery of a potent carbonic anhydrase inhibitor by in silico target fishing.* ACS chemical biology, 2015. **10**(9): p. 1964-1969.
129. Cau, Y., et al., *Potent and selective carboxylic acid inhibitors of tumor-associated carbonic anhydrases IX and XII.* Molecules, 2018. **23**(1): p. 17.
130. Livak, K.J., J. Marmaro, and J.A. Todd, *Towards fully automated genome–wide polymorphism screening.* Nature genetics, 1995. **9**(4): p. 341-342.
131. Naldini, A., et al., *Identification of a functional role for the protease-activated receptor-1 in hypoxic breast cancer cells.* European Journal of Cancer, 2009. **45**(3): p. 454-460.
132. Albini, A., et al., *A rapid in vitro assay for quantitating the invasive potential of tumor cells.* Cancer research, 1987. **47**(12): p. 3239-3245.
133. Rossi, S., et al., *TNF-alpha and metalloproteases as key players in melanoma cells aggressiveness.* Journal of Experimental & Clinical Cancer Research, 2018. **37**(1): p. 1-17.
134. Hess, A.R., et al., *Focal adhesion kinase promotes the aggressive melanoma phenotype.* Cancer research, 2005. **65**(21): p. 9851-9860.
135. O'Reilly, K.E., et al., *Hedgehog pathway blockade inhibits melanoma cell growth in vitro and in vivo.* Pharmaceuticals, 2013. **6**(11): p. 1429-1450.
136. Taghizadeh, H., et al., *Targeted Therapy Recommendations for Therapy Refractory Solid Tumors—Data from the Real-World Precision Medicine Platform MONDTI.* Journal of personalized medicine, 2020. **10**(4): p. 188.